Zhang et al-2016-Geological Journal SI (pp490-512)

Data · September 2016

GEOLOGICAL JOURNAL
Geol. J. **51**(S1): 490–512 (2016)
Published online 2 June 2016 in Wiley Online Library
(wileyonlinelibrary.com). DOI: 10.1002/gj.2807

Origin of transform faults in back-arc basins: examples from Western Pacific marginal seas

Y. ZHANG[1,2], S. Z. LI[1,2,3]*, Y. H. SUO[1,2], L. L. GUO[1,2], S. YU[1,2], S. J. ZHAO[1,2], I. D. SOMERVILLE[4], R. H. GUO[1,2], Y. B. ZANG[1,2], Q. L. ZHENG[1,2] and D. L. MU[1,2]

[1] *College of Marine Geosciences, Ocean University of China, Qingdao, China*
[2] *Key Lab of Submarine Geosciences and Prospecting Techniques, Ministry of Education, Qingdao, China*
[3] *Laboratory for Marine Geology, Qingdao National Laboratory for Marine Science and Technology, Qingdao, China*
[4] *School of Earth Sciences, University College Dublin, Dublin 4, Ireland*

Transform faults in back-arc basins are the key to revealing the evolution of marginal seas. Four marginal basins in the Western Pacific, i.e. the South China Sea (SCS), Okinawa Trough (OT), West Philippine Basin (WPB) and Shikoku-Parece Vela Basin (SPVB), were studied to redefine the strikes and spatial distribution of transform faults or fracture zones. Based on high-resolution tectonomorphology, gravity and magnetic anomalies, pattern of magnetic lineations, seismic profiles, geometry of basins and palaeomagnetic data, together with analyses of regional geological setting, plate reconstruction and geodynamic analysis, this paper suggests that all the transform faults in the four marginal basins are in general NNE-trending. Moreover, by comparing with the contemporary structural framework of the East Asian Continental Margin, we propose new models concerning marginal seas spreading and have revised the previous Cenozoic plate reconstruction models related to the East Asian Continental Margin and the Western Pacific marginal seas. There are three possible origins of these NNE-trending transform faults. 1. Inheriting the orientation of the strike-slip faults at the rifting continental margin (e.g. the SCS and OT). The real strike of transform faults should not be NW but NNE. The large-scale NNE-trending dextral strike-slip faults distributed in the continental shelf of the SCS control a series of pull-apart basins of the SCS. Due to a higher degree of pull-apart, oceanic crust began to open. Then they evolved into the NNE-trending transform faults in the SCS and could also be regarded as a natural extension of the NNE-trending strike-slip faults in the South China Block (SCB). The geodynamic mechanism of the OT is similar to that of the SCS. Consequently, transform faults of the OT should also be NNE-trending, which is not perpendicular to the spreading axis but instead displays oblique spreading. 2. Izu-Bonin-Mariana (IBM) Trench retreat to the NNE and NE. Subduction rollback to the NE and NNE produced the NE- and NNE-striking horizontal tensile stress, resulting in the rifting of the Kyushu-Palau Ridge (KPR), controlling the spreading of the SPVB and forming the NE- and NNE-trending transform faults. This also involves oblique spreading. 3. The later overall rotation of the Philippine Sea Plate (PSP). Since 25 Ma, the WPB has rotated clockwise about 40°. Therefore the NW- and NNW-trending transform faults that formed at the later spreading stage have rotated to be the near-N–S- or NNE-striking faults. These transform faults are almost perpendicular to the spreading axis.

Received 19 November 2015; accepted 10 March 2016

KEY WORDS Western Pacific; marginal sea; transform fault; dextral strike-slip fault; plate reconstruction; plate rotation; subduction rollback

1. INTRODUCTION

The origin of transform faults has not been yet explained completely by the plate tectonics theory. Nonetheless, with the rapid progress of computer technology, some numerical simulation methods have been adopted to investigate the formation of the transform faults in recent studies (Gerya, 2010, 2012; Püthe and Gerya, 2014). However, most of these researches still focused on the formation mechanism of transform faults in the mid-oceanic ridge. The formation and evolution of transform faults in the back-arc basins are still unclear. The back-arc basin transform faults play a critical role in understanding the evolution of marginal seas, and the mechanism of its formation has always been problematic and a hotspot issue in geosciences. The strike of transform faults generally represents the direction of plate motion, which thus can be used to study the dynamics of the evolution of marginal sea basins. This will be helpful in understanding the interaction between the continental plate and oceanic plate at the oceanic-continental transition/subduction zone, and also helpful in reconstructing the tectonic framework and evolution of the

*Correspondence to: S. Z. Li, Department of Marine Geology, College of Marine Geosciences, Ocean University of China, No. 238, Songling Road, 266100, Qingdao, China. E-mail: Sanzhong@ouc.edu.cn

East Asian Continental Margin, the Pacific Plate (PP) and the India-Australia Plate since the Cenozoic.

Since the concept of back-arc basins was proposed in the 1970s (Karig, 1971; Packham and Falvey, 1971; Sleep and Toksoz, 1971), the origin of transform faults in the back-arc basins has always been a focus in earth science (Lee *et al*., 1980; Mrozowski and Hayes, 1982; Taylor and Natland, 1995; Okino *et al*., 1998; Deschamps and Lallemand, 2002; Hall, 2002). However, little attention has been paid to the formation of transform faults in the back-arc basin and their roles in the tectonic evolution of the ocean-continent transition zone until very recently. Liao and Gerya (2014) proposed that the splitting history of continental breakup and seafloor spreading was related to the formation of transform faults, and that one possible and widely-proposed mechanism of transform fault formation was related to the inheritance of pre-existing lithospheric weakness. Honza (1995) found that the direction of the spreading axis was usually not traced to the Euler pole and was oblique to the trend of the transform faults in the back-arc basins, which is different from that in the mid-oceanic ridges where ridges were on great circles perpendicular to the trend of the transform faults. Moreover, the phenomenon universally exists in the Western Pacific marginal basins, as well as some intercontinental seas that are spreading, such as the Red Sea, Gulf of Aden and Gulf of California (Bellahsen *et al*., 2003; ArRajehi *et al*., 2010). This indicates that the transform fault formation in back-arc basins is greatly constrained by the tectonic background of the palaeo-plate and the original tectonics or the basement structures. Moreover, this also provides a new insight into the formation of transform faults in the back-arc basins of the Western Pacific, where their formation in different marginal basins may be similar and can be compared.

Aimed at this important scientific problem, and based on the available materials, such as seismic profiles, gravity and magnetic anomalies, magnetic lineations, submarine geomorphology, basin structural geometry and combined with region geological settings, we redefine the distribution, especially the trend, of transform faults in the SCS, OT, WPB and SPVB. From this we speculate on the possible formation mechanism, and to restore the formation and evolution process of marginal seas in the Western Pacific during the Cenozoic through the insight provided by transform faults according to the previous reconstruction models.

2. GEOLOGICAL SETTING

The Western Pacific active continental margin is in a unique tectonic position, located at the intersection of the three major plates, i.e. the Eurasian Plate (EP), PP and India-Australia Plate, and is one of the most active areas of modern tectonic activity (Li *et al*., 2012; Niu *et al*., 2015). Since the Cenozoic, it has been simultaneously affected by a series of complicated tectonic superposition that formed the world's most significant trench-arc-basin system under the tectonic setting of seaward subduction retreat from west to east. These activities include the following: the indentation of the Indian Plate to the EP, the subduction rollback of the PP and the indentation of the PSP along the Taiwan Orogenic Belt (Maruyama *et al*., 2009; Dai *et al*., 2014). It concentrates about 75% of the marginal seas in the world (Tamaki and Honza, 1991), from north to south, or from west to east, and includes the following: the Okhotsk Sea (50-14 Ma), Japan Sea (28-15 Ma) and OT (2 Ma-present-day) and SCS (34-16 Ma), Sulu Sea (20-15 Ma), Celebes Sea (48-35 Ma), WPB (54-33 Ma) and SPVB (30-17 Ma), and Caroline Sea (38-27 Ma) (Fig. 1). This paper focuses on transform faults in the WPB, SCSB, SPVB and OT to carry out some further work.

2.1. *The SCS*

The SCS is surrounded by the China mainland to the north, Philippines to the east, Kalimantan (Borneo) to the south and Indochina Peninsula to the west. The total area of the SCS is about $350 \times 10^4\,km^2$, and the maximum depth reaches 5559 m (Luan and Zhang, 2009). It is known as the largest and deepest marginal sea around the East Asian Continental Margin (Fig. 1).

The SCS is enclosed by four different types of continental margins. The northern margin has been generally considered to be a passive continental margin since the Miocene. The southern part is the subduction-collision belt along the Nansha Trough. The eastern part is the Manila Trench (MT) which is still active currently, and the western part is the N–S-trending large-scale strike-slip fault zone (Red River Fault Belt) (Fig. 1). According to the water depth data and the characteristics of submarine topography and geomorphology, the SCS can be divided into three sub-basins: the NW Sub-basin, the Central Sub-basin and the SW Sub-basin, which display a roughly SW-trending extensional 'V' shape.

The SCS was greatly controlled by the Tethyan tectonic domain in its geological history, experiencing the complicated tectonic evolutionary processes. The continental crust collapsed and was dismembered in its northern margin, and then the southern part involved exotic terrain amalgamation and continental accretion. Oceanic crust was generated in the middle part of the SCS and then subducted beneath the MT to the east (Fu *et al*., 2007).

2.2. *The OT*

The OT is an elongated crescentic depression oriented in a general NE–SW direction, which is located between the

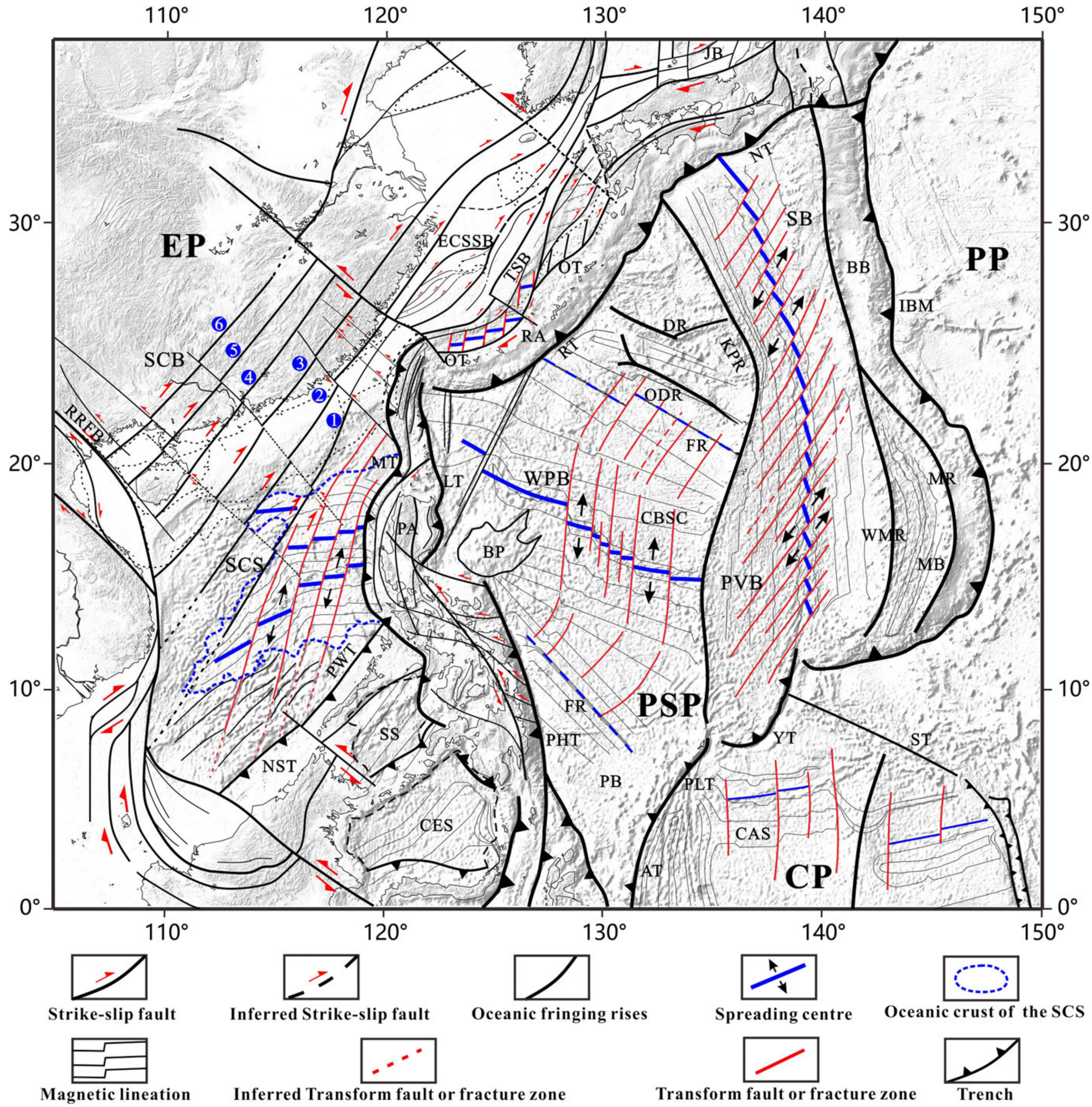

Figure 1. Tectonic units of the Western Pacific and East Asian Continental Margin. Abbreviations: PP, Pacific Plate; NT, Nankai Trench; SB, Shikoku Basin; IBM, Izu-Bonin-Mariana Trench; BB, Bonin Basin; MR, Mariana Ridge; MB, Mariana Basin; PVB, Parece Vela Basin; CP, Caroline Plate; CAS, Caroline Sea; AT, Ayu Trough; PLT, Palau Trench; YT, Yapu Trench; PB, Palau Basin; PSP, Philippine Sea Plate; BP, Benham Plateau; FR, Fossil Ridge; PHT, Philippine Trench; CBSC, Central Basin Spreading Centre; WPB, West Pacific Basin; LT, Luzon Trench; ODR, Oki-Daito Ridge; DR, Daito Ridge; KPR, Kyushu-Palau Ridge; RT, Ryukyu Trench; RA, Ryukyu Arc; OT, Okinawa Trench; JB, Japan Sea Basin; TSB, Taiwan-Sinzi Belt; ECSSB, East China Sea Shelf Basin; EP, Eurasian Plate; RRFB, Red River Fault Belt; SCB, South China Block; SCS, South China Sea; PWT, Palawan Trench; NST, Nansha Trough; SS, Sulu Sea; CES, Celebes Sea; MT, Manila Trench; PA, Philippine Arc. Fault name: 1. Binhai Fault; 2. Changle-Nanao Fault; 3. Zhenghe-Dapu Fault; 4. Shaowu-Heyuan-Yangjiang Fault; 5. Wuchuan-Sihui Fault; 6. Chenzhou-Bobai-Hepu Fault.

Ryukyu Arc and the East China Sea Shelf Basin (ECSSB), about 1200 km in length (Fig. 1). To the west of the OT is the Taiwan–Sinzi Belt separating the OT from the ECSSB (Suo *et al*., 2015). The PSP is subducting northwestwards beneath the EP (Li *et al*., 2013; Liu *et al*., 2013, 2014), and the OT represents an initial back-arc basin formed

DOI: 10.1002/gj

behind the Ryukyu Trench and Ryukyu Arc. The OT can be divided into three segments: the northern Tokara Depression, the central Iheya Depression, and the southern Trough Depression (Liu *et al*., 2016). Linear magnetic anomalies were tracked in the axial section of the central segment of the OT (Liang *et al*., 2001). Meanwhile, tholeiitic basalts were found in the middle and southern segments of the OT (Shinjo and Kato, 2000). This suggest that there is ridge spreading in the central rift zone in the middle and southern segments of the OT, with new oceanic crust growth and magma arising. In addition, by comparing the initial oceanic crust thickness, heat flow and hydrothermal activity in the global passive continental margins and marginal seas in the Western Pacific with those in the OT, Liu *et al*. (2016) proposed that the southern and central parts of the OT were at the initial stage of seafloor spreading, while the northern part was still in the continental breakup stage and had the characteristics of transitional crust.

2.3. The PSP

The PSP has a roughly diamond-like shape, long in a N–S direction and short in an E–W direction, consisting of the WPB and the SPVB, covering an area of about $54 \times 10^6\,\mathrm{km}^2$. It is sandwiched between the EP and the PP, almost entirely surrounded by a deep trench, and to the south is the India-Australia Plate (Qu *et al*., 2007; Wu *et al*., 2013) (Fig. 1). The eastern boundary comprises, from north to south, the IBM Trench, Yap Trench, Palau Trench and Ayu Trough, successively. The PP is subducting beneath the PSP along the IBM Trench (Takahashi *et al*., 2007). The Yap Trench, Palau Trench and Ayu Trough are the tectonic boundaries separating the Caroline Plate from the PSP (Fujiwara *et al*., 1995). The western boundary comprises, from north to south, the Nankai Trough, Ryukyu Trench, MT and Philippine Trench, successively. Along the Nankai Trough, the Ryukyu Trench and the Philippine Trench, the PSP is subducting beneath the EP (Tokuyama, 1995). The SCS is subducting beneath the PSP at the MT. The Philippine Fault and its secondary faults are well developed and run through the whole Philippine Arc, displaying a left-lateral strike-slip property, regulating the transitional relationship between the two subduction zones (Xue *et al*., 2012). The southern boundaries are made up of the Philippine Trench, the Molucca Fault Zone, the Halmahera Trench and the Saorong Fault Zone.

Based on the new seafloor topography data and available K/Ar and Ar/Ar ages, Deschamps and Lallemand (2002) re-examined Hilde and Lee's (1984) model and proposed that the WPB is a back-arc basin where seafloor spreading occurred from 54 to 33 Ma, with a possible later magmatic activity at the ridge axis between 28 and 15 Ma. Data and models by Hall *et al*. (1995a, b), which were subsequently modified by Deschamps and Lallemand (2002) and Queano *et al*. (2007), amongst others, and recent palaeomagnetic data by Yamazaki *et al*. (2010) suggested an up to 90° clockwise rotation of the PSP since the Middle Eocene, with about 15° northward migration of the WPB. The ridge orientation of the Shikoku Basin (SB) underwent a gradual transition from NNW to NW, and there is a seamount chain in the central SB, namely the Kinan Seamount Chain. There is a central rift named the Parece Vela in the Parece Vela Basin (PVB), and the rift is supposed to be a spreading centre (Wu *et al*., 2013). Studies indicated that the SB, PVB and Mariana Trough all propagated from west to east successively (Karig, 1971, 1975; Uyeda and McCabe, 1983; Seno and Maruyama, 1984).

3. NNE- OR NEAR-S–N-TRENDING TRANSFORM FAULTS IN THE WESTERN PACIFIC MARGINAL SEAS

The strikes of transform faults can directly represent the plate motion direction, which has a very important kinematic significance in revealing the formation and evolution of marginal seas. Therefore, to realize the opening direction of marginal seas, we must first redefine the strikes of the transform faults.

3.1. Revision of transform faults in the SCS

Transform faults of the SCS cut through the Moho surface. They are reformed by the later massive intraplate volcanism and the giant NW-trending strike-slip fault sets. Submarine geomorphology, gravity and magnetic anomalies, and magnetic lineations are applied to redefine the strikes of transform faults in the SCS, although there are few seismic profiles across the three sub-basins.

3.1.1. Analysis of the fine submarine geomorphology in the SCS

Analysis of the submarine tectonomorphology is an important approach to exploring the characteristics of the young seafloor tectonics. Since the 1990s, the high-resolution multi-beam seafloor topography and geomorphology detection technology has been widely applied in the study of seafloor spreading. By comparing submarine topography with the deep geological information obtained by the gravity and magnetic anomalies, and seismic profiles, many achievements have been made in the study of mid-oceanic ridge spreading. Loureneo *et al*. (1998) introduced this method to geodynamic research on the triple junction in the Azores of the Atlantic Ocean amongst the American, European and African plates.

DOI: 10.1002/gj

The geometry of marginal seas is not only restricted by small structures inside the basin but also controlled by the large-scale faults in the basin margin. The SCS is a wedge-shaped basin, which is wide in the NE and narrow in the SW, like a NE-axial rhombus in plan view (Fig. 2). From simple kinematic analysis, the opening and spreading of the SCS as a pull-apart basin were strongly influenced by the NNE-trending dextral strike-slip faults (Li *et al*., 2012), which were similar to the opening and spreading of the Japan Sea (Yin, 2010). Their spreading is asymmetric, which is wide in the east and narrow in the west. The spreading rate in the east was significantly larger than that in the west. A large number of NE-trending linear structural belts, such as cliffs and broken-walls, were recognized by the high-resolution multi-beam submarine geomorphology. These structural belts were concentrated between 17° and 14° N and were greatly reformed by the later NW-trending strike-slip faults. From the statistical results, a strike of NE 67° is the dominant strike of these strike-slip faults (Li *et al*., 2002). These NE- and ENE-trending linear structural belts are discontinuous along strike, with a clumped and zonal distribution of numerous minor secondary faults controlled by the major NNE-trending dextral strike-slip faults. The comparison results between the linear submarine tectonomorphology and deep geological information by seismic profiles show that submarine surface structures, such as cliffs and broken-walls, have a good correlation with faulted block configuration. In fact, the submarine surface structure was a reflection of basement-involved faults during the spreading. This eliminated the possibility that surface structures developed in the neotectonics after spreading (Taylor and Hayes, 1983).

In addition, there are many isolated submarine volcanoes along the NNE-trending linear structural belts as shown in Figure 2. The mantle-derived basaltic melts could migrate along the lithosphere-scale faults to the upper oceanic crust (Hui *et al*., 2016b), which is the most direct geological record for the oceanic crustal evolution. These volcanoes developed probably under the intraplate volcanism along the strikes of transform faults after the cessation of spreading of the SCS (Yan *et al*., 2008; Shi and Yan, 2013). Therefore, the NNE-trending fault belts are the transform faults of the SCS.

3.1.2. Gravity and magnetic anomalies in the SCS

The characteristics of basement faults can be clearly distinguished by the gravity and magnetic anomaly features. The third-order details of Bouguer anomalies by the wavelets (Fig. 3) can reflect the whole characteristics of gravity anomaly. Therefore, gravity and magnetic anomalies are significantly important pathways to reveal the deep-seated faults in the sea area.

A series of NE- and NNE-trending strike-slip faults are distributed in the SCB and continue to extend southwards to the northern continental margin of the SCS (Fig. 1). Then they become the basin boundary of the northern continental shelf of the SCS, or separated the secondary depressions inside the basin (Ma *et al*., 2014; Wang *et al*., 2014). Some of them cross the nearly equiaxial high gravity anomalies, and some are situated in the boundary between positive and negative gravity anomalies with amplitudes from −10 to +10 mGal. A few are located in the boundary of the NE-trending long-axis gravity anomaly, which indicated the strike of faults. The positive and negative gravity anomalies alternate from west to east, consistent with the alternating arrangement of the uplifts and depressions in the northern SCS and with the fault pattern in the northern SCS and the SCB (Li *et al*., 2012).

In the oceanic crust of the SCS, most of the fault zones pass through the equiaxial high gravity anomalies. Some are along the linear gradient belt of the gravity anomaly, which is the boundary between the high and low gravity anomalies. The NE- and NNE-trending strike-slip faults are all clearly reflected in the boundary of the positive and negative magnetic anomalies. There exists numerous long-axis gravity anomalies closely parallel to the spreading axis. The horizontal offset of these long-axis gravity anomalies shows that the NE- and NNE-trending faults are dextral. The NE- and NNE-trending strike-slip faults correspond well to gravity and magnetic anomalies (Figs. 3 and 4).

In the southern SCS, the string of beads or bullseye positive gravity anomalies are very obvious along the fault zones, with the NNE-trending arrangement and the highest positive anomaly up to 20 mGal, which are well distinct from the whole negative anomaly in this area (Fig. 3). After the cessation of spreading of the SCS, the later massive intraplate volcanism in this sea area was active and strong, and the magma migrated to the seafloor along the earlier formed lithosphere-scale faults (Hui *et al*., 2016b), resulting in the disordered magnetic anomaly that has obvious fluctuations in the positive and negative magnetic fields.

In summary, the NE- and NNE-trending strike-slip faults in the SCB extend to the northern slope of the SCS, pass through the oceanic crust of the SCS and further develop in the southern margin of the SCS (Fig. 3). Furthermore, the NE- and ENE-trending strike-slip faults are widely distributed in the whole of the SCS and also are consistent in strike of the transform faults at the SCS spreading.

3.1.3. Magnetic lineations in the SCS

Significant obvious magnetic lineations exist in the SCS (Figs. 1 and 2). Magnetic lineations used in our study are obtained from the Earth Byte Team in the University of Sydney (http://www.earthbyte.org/). Magnetic lineation in the Central Sub-basin of the SCS is nearly E–W-trending in strike,

DOI: 10.1002/gj

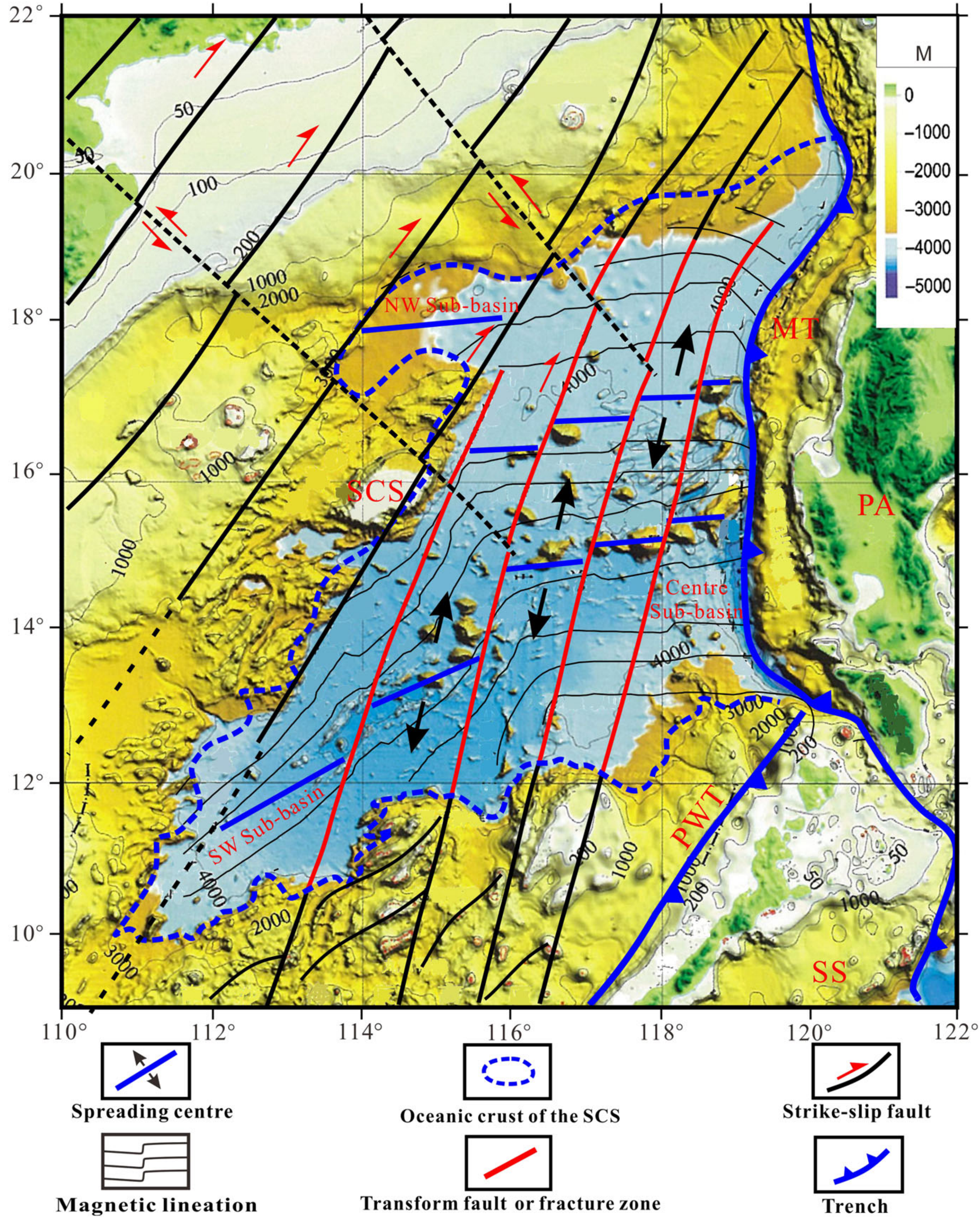

Figure 2. Precise submarine geomorphology in the SCS (revised from Chen and Wen, 2010) and distribution of faults (see Fig. 1 for abbreviations).

DOI: 10.1002/gj

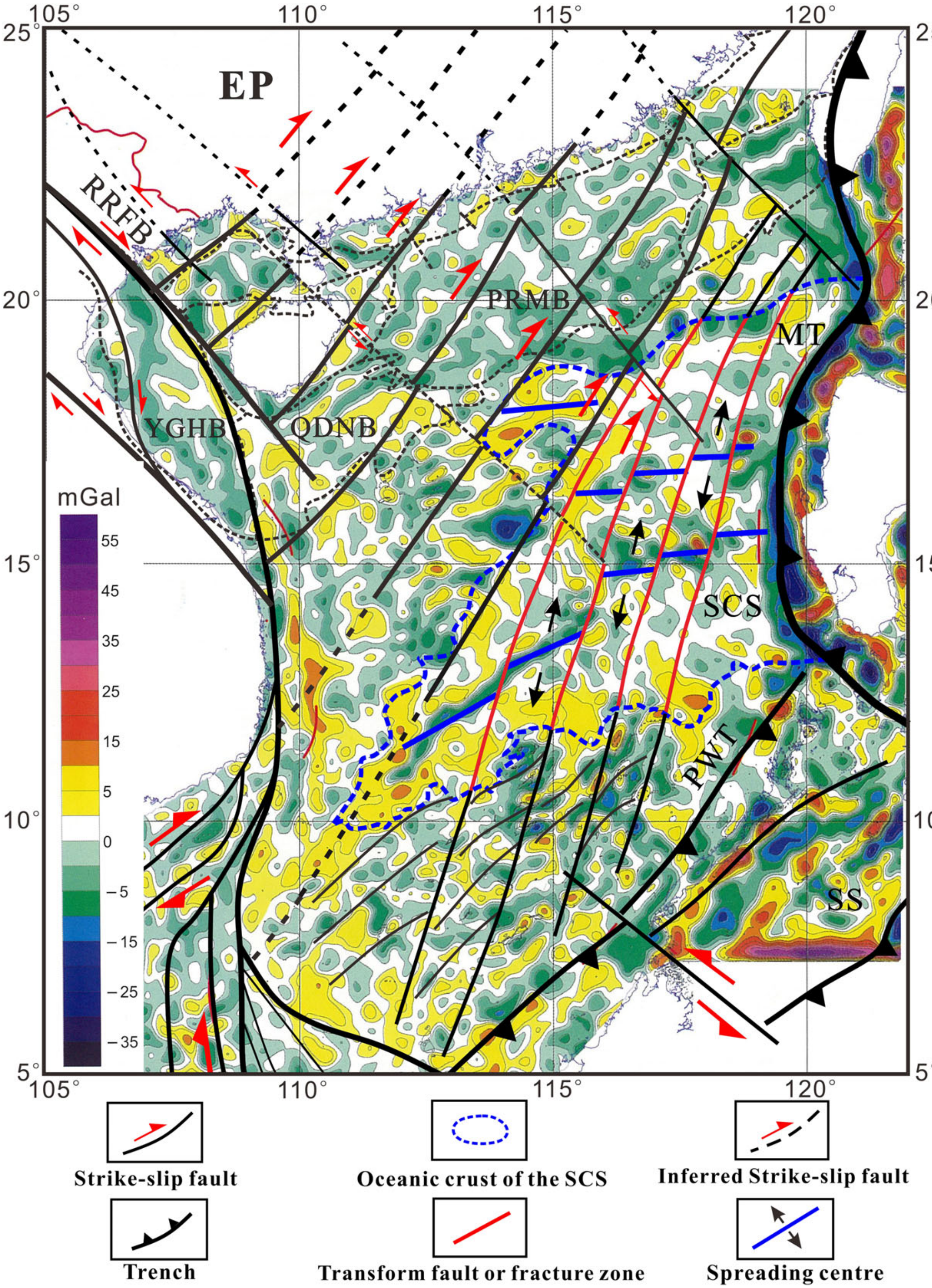

Figure 3. Third-order details of Bouguer anomalies by the wavelets (gravity data form Chen and Wen, 2010) and the fault distribution in the SCS. Abbreviations: PRMB, Pearl River Mouth Basin; QDNB, Qiongdongnan Basin; YGHB, Yinggehai Basin; SCS, South China Sea; RRFB, Red River Fault Zone. For other abbreviations, see Figure 1.

DOI: 10.1002/gj

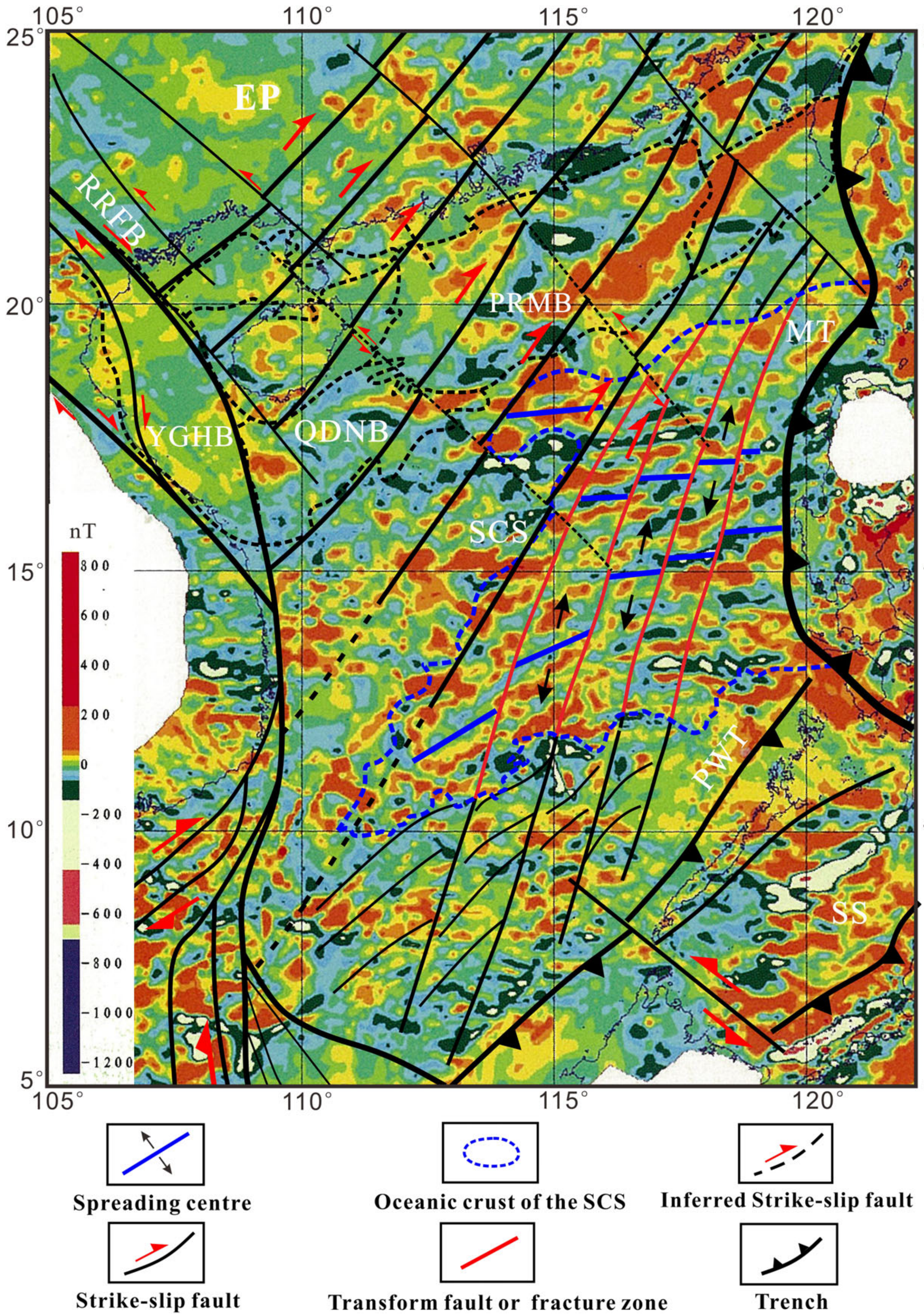

Figure 4. Magnetic anomaly (magnetic data from Zhu and Mi, 2010) and fault distribution in the SCS (see Fig. 3 for abbreviations).

DOI: 10.1002/gj

almost parallel to the spreading axis, while magnetic lineations in the SW Sub-basin are slightly oblique to the spreading centre (Fig. 2).

The vertical distance between the adjacent magnetic lineations is not the same, indicating the different spreading velocities at different stages. The magnetic lineation as a whole was curved or offset at intervals at the intersection between the magnetic lineation and a transform fault. It is discontinuous in strike. The orientation of the line collecting the nearest nodes at the adjacent magnetic lineations is NNE-trending, showing the strike of the transform fault (Fig. 2) and indicating the spreading direction of the SCS. The magnetic lineation between the adjacent transform faults still has good correlation and continuity in space and is horizontally offset into several sections by the NNE-trending transform faults. By comparing the magnetic lineations, we can precisely analyse the differences in spreading rate between the SW Sub-basin and the Central Sub-basin. In addition, the previous NE- and NNE-trending dextral strike-slip faults are the predecessors of transform faults.

In conclusion, all kinds of features point out that the true strikes of the transform faults in the SCS are NE or NNE, including the NE- and NNE-trending linear fault zones, the intraplate volcanism along the lithosphere-scale faults, the NNE-trending gradient zones of gravity and magnetic anomalies, the string of beads or bullseye anomalies, and the structures of magnetic lineation.

3.2. *The characteristics of transform faults in the PSP*

Extensive investigations concerning the transform faults of the WPB and the SPVB in the PSP have been made in the past decades. Based on magnetic lineation, gravity and magnetic anomalies, tectonic geomorphology in the seafloor and other methods, it was recognized that the early spreading direction of the WPB was NE-trending, while the late spreading stage was nearly N–S- or approximately NNE-trending, and that the transform faults of the SPVB were NNE-trending at the late spreading stage.

3.2.1. *Transform faults in the WPB*

Many cruises of the Ocean Drilling Program (ODP) have been conducted in the vicinity of the Central Basin spreading centre of the WPB since 1984, and a good deal of data about the bathymetry, magnetic and gravity anomalies have been collected (Oshima *et al*., 1988; Lallem and Liu, 1997; Deschamps *et al*., 1999; Fujioka *et al*., 1999; Okino *et al*., 1999; Fujioka *et al*., 2000; Okino and Fujioka, 2003). Based on these data, extensive and detailed researches were carried out concerning the spreading history of the WPB.

The strikes of the fracture zones are believed to be parallel to the spreading direction at the time of formation for most spreading ridges (Wilson, 1965). Abyssal hills were usually perpendicular to the strike of the fracture zones (Luyendyk, 1969; Andrews, 1976). According to the tectonic geomorphology provided by the long-distance side-scan sonar mapping (Swathmap), Andrews (1980) confirmed the linear abyssal hills south of the Central Basin Fault in the WPB are parallel or subparallel to the extinct or fossil spreading centre, known as the Central Basin Fault Zone. Therefore, the spreading direction of the WPB could be judged by the distribution of the abyssal hills. The early seafloor spreading direction of the WPB was NE-SW initially and reoriented later to near-N–S-trending (Andrews, 1980).

Analysing the magnetic lineations and the seafloor spreading structures, Hilde and Lee (1984) proposed that the WPB developed in two stages. The first stage was between 58 and 45 Ma, and the spreading was in a NE–SW direction with a half spreading rate of 44 mm/yr, and the second stage was from 45 to 33 Ma and characterized by a N–S-directed spreading at a rate as slow as 18 mm/yr. In addition, the former NW–SE Central Basin spreading centre was separated into numerous, short, nearly E–W-trending spreading segments by N–S-trending transform faults or non-transform discontinuities. These preliminary works on magnetic lineations were widely adopted in researches concerning the spreading process of the WPB (Hall *et al*., 1995a, b, c; Deschamps and Lallemand, 2002; Hall, 2002; Sasaki *et al*., 2014).

Based on the analysis of the tectono-magmatic processes, Deschamps *et al*. (2002) pointed out that the initiation of the PVB E–W-trending spreading took place 30 Ma later than the termination of the WPB spreading and that extensive stresses within the PVB were probably transmitted to the hot and easily deformable rift valley of the WPB and thereby formed a NE–SW-trending extension stress field. This led to the creation of a new NW–SE axis in place of the former E–W-trending spreading system, that is, the spreading centre in the late nearly N–S spreading stage of the WPB was almost in an E–W direction (Fig. 1).

3.2.2. *Transform faults in the SPVB*

Sdrolias *et al*. (2004) achieved much work on the SPVB, determining the strikes of spreading ridges, and confirmed the tectonic geomorphology of the spreading centre and submarine fault zones utilising the available bathymetric and gravity anomaly data. The spreading axis strike of the SB switched from NNW-trending in the north to NW-trending in the south, connecting the NW-trending spreading ridges in the PVB. The change in the strikes of the magnetic lineations and fracture zones can indicate a change in the strikes of transform faults, which reflects that the spreading was reorientated. About 20 Ma ago, the spreading direction of the PVB switched from E–W to NE–SW, while the SB changed from ENE–WSW to NE–SW or NNE–SSW. This conclusion was widely accepted.

According to the distribution of magnetic lineations (Fig. 1) and characteristics of free-air gravity anomalies (Fig. 5) in the PSP, combined with the seafloor spreading structures, this paper also reaches the same conclusions as the earlier study (Sdrolias *et al*., 2004). Therefore, there are two spreading stages in the WPB: the first in a NE–SW direction and the later stage changed to NNE–SSW.

4. THE MODELS AND BACKGROUND OF TRANSFORM FAULT FORMATION IN MARGINAL SEAS

4.1. The SCS and OT: the model of inheriting the orientation of strike-slip faults at the divergent continental margin and adjacent regions

4.1.1. The two popular models of the opening of the SCS

There are a variety of controversial plate reconstruction models about the opening of the SCS. But the two main models are called the subduction model (Holloway, 1982; Hall, 2002) and extrusion model (Briais *et al*., 1993).

In the *subduction model*, the proto-SCS subducted under the Kalimantan Block with a low angle, and the drag effect resulted in the opening of the SCS. The Kalimantan Block rotated counter-clockwise, the subducting oceanic crust of the proto-SCS vanished and ultimately the continent-continent collision occurred between the Dangerous Block and the Kalimantan Block. The existence of the proto-SCS oceanic crust has provided a reasonable explanation for the evolution of the Rajang-Crocker accretionary wedge, the volcanic activity of the Sabah-Cagayan Ridge and the space for the spreading of the SCS. However, this model has some major problems. It cannot explain the phenomenon of the nearly E–W-trending magnetic lineation that exists in the Central Sub-basin of the SCS (Fig. 2). In addition, the proto-SCS is very narrow, and its subduction amount is not sufficient to drive the SCS to open (Xu *et al*., 2014). Moreover, it also does not explain the fact that rifting occurs concurrently in the ECSSB adjacent to the SCS (Zhou *et al*., 2002), which does not favour a unified dynamic mechanism of the marginal seas widely distributed in the Western Pacific.

In the *extrusion model* of Briais *et al.* (1993), there was no proto-SCS subduction zone on the northwest side of the Kalimantan Block, the collision between the Indian Plate and the EP accelerated the extrusion and escape of Indochina and other blocks on both sides of strike-slip faults, accompanied by a rotational motion. The related left-lateral pull-apart effect eventually led to the SCS to open and expand, and the clockwise rotation of the Kalimantan Block developed coevally. However, this model created a huge controversy; the basic theory and the physical model were not in conformity with the facts. The SCS is a wedge-shaped basin; it is not consistent with the left-lateral pull-apart mechanism of the southeastern end of the NW-trending Red River Fault Zone (RRFZ) (Zhou *et al*., 2002; Fig. 1). Li *et al*. (1998) pointed out that the Yinggehai Basin was formed by the RRFZ extending at the SCS, and that the RRFZ had been not left-lateral but right-lateral since the Eocene. This indicates that the Ailaoshan-RRFZ did not affect the SCS. According to the new $^{40}Ar/^{39}Ar$ data, Wang *et al*. (2000) proposed a sinistral motion of the Ailaoshan-RRFZ that occurred at 27.15 Ma, later than the opening time of the SCS, indicating that the extrusion tectonics cannot be the true cause for the initial opening of the SCS. Dewey *et al*. (1989) believed that the huge energy that the Indian Plate indented into the EP was mainly consumed by the uplift of the Tibetan Plateau, while the Indochina Block slipped only a short distance. In addition, palaeomagnetic studies showed that coeval clockwise rotation rather than counter-clockwise rotation had taken place in the Kalimantan Block (Hutchison, 2010).

In summary, we don't believe that these two models are reasonable explanations for the spreading of the SCS.

4.1.2. The pull-apart effect of the NNE-trending right-lateral strike-slip faults in the formation mechanism of the SCS

There are many disputes in the distribution and direction of the magnetic lineation of the SCS. Li (2011) considered that the SCS experienced two different stages of spreading with distinct directions: the early NNW–SSE-directed spreading occurred between 33.5 and 25 Ma, forming the older oceanic crust of the NW Sub-basin and somewhere away from the Central Sub-basin, with the nearly E–W- and ENE-trending magnetic lineation, while the late NE–SW-directed spreading occurred between 23.5 and 16.5 Ma, forming the new oceanic crust of the SW Sub-basin and somewhere nearby the Central Sub-basin with the approximate NE-trending magnetic lineation. However, most studies suggested the magnetic lineations in the Central Sub-basin were nearly E–W-trending during 25-16 Ma (Taylor and Hayes, 1983), in which the SW Sub-basin and the Central Sub-basin were spreading meantime. Apparently, it is impossible for two different stress fields to exist simultaneously at the same stage in the same region under the same geodynamic setting. That is to say, it is out of the question that the SW Sub-basin of the NW–SE-directed spreading could not occur coevally along with the Central Sub-basin of S–N-directed spreading. Moreover, the equally-spaced, NW- and NNW-trending sinistral strike-slip faults that penetrated throughout the whole region later (Yeh *et al*., 2010) were well preserved and easily identified. These strike-slip faults were often misunderstood as the transform faults cutting off the spreading axis of the SCS, which led to some researchers concluding that the

DOI: 10.1002/gj

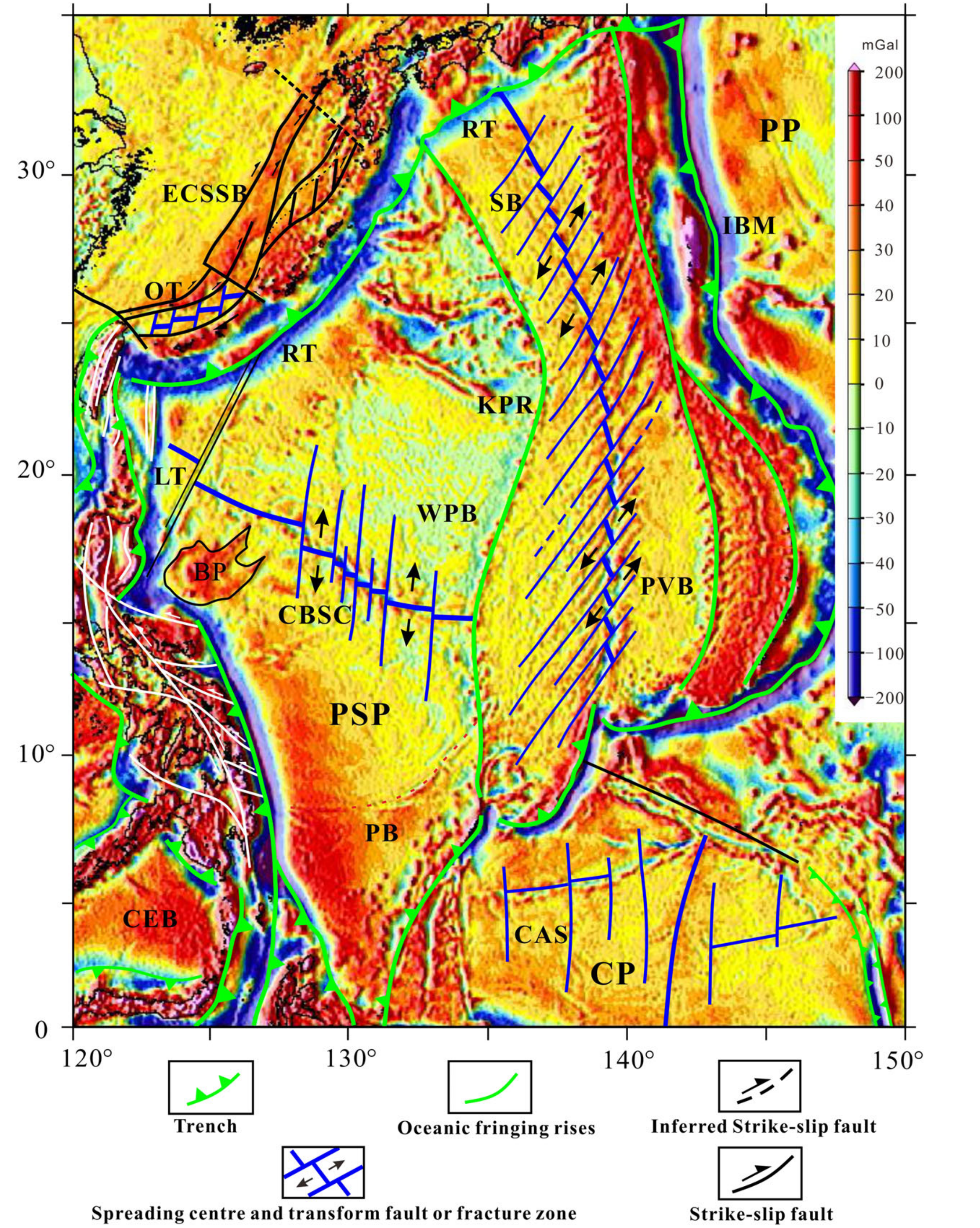

Figure 5. Free-air gravity anomaly of the Philippine Sea Plate. Abbreviations: CBSC, Centre Basin Spreading Centre. For other abbreviations, see Figure 1. White lines in the Philippines and Taiwan represent faults. Gravity anomaly data from Bureau Gravimétrique International (BGI); the resolution is 2′ × 2′.

SCS experienced two spreading stages under different spreading directions of two successively different spreading events or gradual propagation spreading to explain the opening process of the SCS. Furthermore, if the transform faults of the SW Sub-basin were NW-trending, the way how the mid-oceanic ridge broke through the constraints of transform faults to grow up progressively southwestward should be studied further. It is also worth considering further how different segments of the spreading centre are connected. Therefore, the current research results did not neglect the scissor-like opening model of the SCS. Thus, the SW Sub-basin and the Central Sub-basin are possibly under the same unified geodynamic mechanism.

The evolution of the SCS (Fig. 1) was significantly influenced by the right-lateral strike-slip faults, similar to those of the Japan Sea. The dextral strike-slip pull-apart effect was characterized as intensive in the east, weak in the west and acting earlier in the north and the east than in the south and the west, in a different shearing extent. Then, the difference in the degrees of shearing in the same period in different tectonic domains can explain the inconsistency of the magnetic lineations between different right-lateral strike-slip faults, and also interpret the inconsistency of the magnetic lineations belonging to the same mid-oceanic ridge segments in different periods. Furthermore, the formation mechanism of the SCS is similar to the Late Cretaceous basins in the SCB, the northern shelf basins of the SCS and the ECSSB.

Jolivet *et al.* (1994) found that there existed one large right-lateral strike-slip shear fault zone at the eastern and southwestern edges of the Japan Sea, respectively. Their displacements reached 400 km and 200 km, respectively. The eastern side of the shearing displacement is much larger than the left one. These two giant dextral strike-slip shear zones were active during the Late Oligocene to Middle Miocene, coeval to the opening time of the Japan Sea. The Japan Sea was located in a local extensional area at the southern segment of the eastern shear fault zone. Most of the subsequent displacement in the extensional area was accommodated by the spreading of the oceanic crust. Tamaki (1995) believed that it is a common process of back-arc spreading that the lithosphere along the giant strike-slip shear fault zone was torn to trigger seafloor spreading.

The back-arc basin has its own independent spreading system similar to the ocean. Because of the unique location of the continent margin between oceanic and continental crusts, and the complex tectonic settings, the back-arc basin can undergo dramatic changes at a short time, especially influenced easily by the motion of the subducting plates and the pre-existing tectonic framework of the continental margin. Therefore, the complexity and spatial heterogeneity is a common feature of back-arc spreading. In fact, it was because of the constraint of a complex tectonic background that the SCS was not the orthogonal spreading of normal mid-oceanic ridges, but oblique spreading, similar to the Red Sea-Gulf of Aden. The true strike of the SCS transform faults should be NNE-trending, which was the extensional direction since the late Late Cretaceous, accompanied by the NNE-trending right-lateral strike-slip faults in the SCB and the northern SCS (Jolivet and Tamaki, 1992).

A series of NE- and NNE-trending strike-slip faults were widely distributed in the East Asian Continental Margin, along which a large-scale, intensively active, NE- and NNE-trending Andean-type continental magmatic arc developed during the Late Jurassic to early Late Cretaceous. A set of NNE-trending volcanic formations developed from the Okhotsk Sea to the northwestern margin of the SCS (Zhao and Ohtani, 2009). Since the India-Australia Plate and the EP did not collide at this stage, the fault system and magmatic arc might have been caused by the intensive subduction of the palaeo-PP to the EP. The NE- and NNE-trending strike-slip faults in the SCB were more obvious, extending hundreds of kilometres, some even up to several thousand kilometres, cutting through the lithosphere. The main faults from west to east were the Wuchuan-Sihui, the Shaowu-Heyuan-Yangjiang, the Zhenghe-Dapu, the Changle-Nanao, the Binghai and other fault zones (Fig. 1). Due to the influence of the NW-trending oblique subduction of the palaeo-PP in the Early Cretaceous, the NE-trending fault system showed a sinistral transpressional property (Lin, 1999). Maruyama *et al.* (2009) and Suo *et al.* (2012) considered that it was converted to a tensile stress field because of the steepening subduction angles of the PP in the Late Cretaceous and the initial subduction rollback, the nature of the NE-trending fault system changed from transpression to transtension. The NE- and NNE-trending strike-slip faults performed obvious transtension in the Early Paleogene, forming a series of pull-apart basins in the East Asian Continental Margin.

According to gravity and magnetic anomalies, as mentioned above, there existed an extensive series of long and straight NE- and NNE-trending dextral strike-slip faults in the SCS. Based on the focal mechanism solutions and their characteristics, and the tectonic geomorphology, Wang *et al.* (2014) found that the NE- and NNE-trending strike-slip faults in the SCB could be compared with those in the northern SCS. They extended naturally to the continental margin of the northern SCS. The NE-trending fault system in the SCB extended into the sea and continued to grow in the continental margin of the northern SCS, since these faults in the SCB and SCS developed under the same unified geodynamic setting and by a similar formation mechanism. Karig (1971) also proposed that the deep-seated faults in the SCB, such as the Wuchuan-Sihui Fault, extended into the continental margin of the northern SCS. Lin *et al.* (2006) considered that the NE-trending granite uplift zone in Hainan Island was an extension of the tectonic-magmatic

DOI: 10.1002/gj

belt in the SCB to the SCS, and that the Xisha Uplift, Zhongsha Uplift and Dongsha Uplift and others were also controlled by the NE-trending fault system. Cheng *et al.* (2012) supposed that the Binhai Fault Zone had no change in strike and its extension to the sea area was the fault boundary between the Pearl River Mouth Basin and the Southwest Taiwan Basin. The seismic profile is the most useful tool to reveal fault type. From the seismic profiles across the continental shelf of the northern SCS (Fig. 6), it is easy to determine that the NE-trending fault zones are all negative flower structures, indicating that the fault zones are transtensional and cut down to the Mesozoic basement (T7 interface), up to the Quaternary sediments (over the T1 interface). These characteristics are consistent with those of the Zhenghe-Dapu, Shaowu-Heyuan-Yangjiang and Changle-Nan'to fault zones in the SCB, which indicates that there is a connection amongst their origins. On the basis of the above analysis, the NE- and NNE-trending fault zones in the continental margin of the northern SCS are the natural extension of the NE- and NNE-trending strike-slip faults in the SCB.

Before the Oligocene, the southern SCS was also located in the continental margin of South China based on plate reconstruction (Hall, 2002). Basin-controlling faults in the southern SCS were consistent with those present in the northern SCS. The NE- and NNE-trending strike-slip faults were distinct in terms of gravity and magnetic anomalies, cutting thought the Late Cretaceous strata in the seismic profiles. They were consistent with the NE- and NNE-trending fault zones in the SCB, derived from the NE-trending structures since the Yanshanian Movement (Xiong *et al.*, 2012). Based on the gravity and magnetic anomalies (Figs. 3 and 4), the NE- and NNE-trending strike-slip faults originated from the SCB extended and cut the northern continental margin of the SCS, across oceanic crust of the SCS as transform faults or fracture zones, and further to the southern SCS. Consequently, the widely distributed NE- and NNE-trending strike-slip fault zones, which extend far and cut through the basement of the continental shelf in the SCS, might control the rifting, opening or spreading process of the SCS, and switched into the transform faults of the SCS.

Marginal basins generally undergo a long-term extension before spreading. The collision between the Indian and Eurasian plates started in the Early Eocene and became more intense in the Mid-Eocene about 42 Ma. Meanwhile, the motion direction of the PP changed from NNW to WNW (Fig. 7A-7B). All of the above strengthened the large-scale NE- and NNE-trending dextral strike-slip faulting, which resulted in stretching, splitting and thinning of the SCB lithosphere. Eventually, the Dangerous Block and the Zhongsha Block were successively separated from the SCB. The SCS opened in the Early Oligocene and then converted into a passive continental margin at the south and north margins until the Mid-Miocene. The comparison of the spreading times of marginal seas in the Western Pacific with the uplift stages of the Qinghai-Tibet Plateau revealed that the spreading time of most marginal seas was in the Oligocene, which was also the second peak in uplift of the Tibetan Plateau. Therefore, both of them have a direct and close correlation. In addition, P-wave seismic tomography (Huang and Zhao, 2009) has been carried out to explore the mantle structure under the EP. It showed that a large number of lithosphere materials were continuously injected into the mantle along the collision zone of the India-Australia Plate and the EP (Liu *et al.*, 2004) and that low-velocity asthenosphere as mantle flow extruded eastward from the Qinghai-Tibetan Plateau to East China (Li *et al.*, 2013).

Compared with that of the Japan Sea, the model of the SCS by dextral pull-apart rifting of the continental margin has the main difficulty of determining how the subduction convergence zone developed along the MT rather than the large-scale dextral strike-slip faults in the near-N–S-trending eastern margin of the SCS (Zhou *et al.*, 2002). However, palaeomagnetic evidence suggests that the Philippine Archipelago migrated along the sinistral strike-slip faults from the equator to the present-day location. The strike-slip faults in the eastern margin of the SCS might be destroyed by the following obduction of the Philippine Archipelago, or subducted under the OT with the northward migration of the PSP (Zhou *et al.*, 2002). Xu *et al.* (2014) also proposed that the large-scale dextral strike-slip faults possibly existed in the near-N–S-trending eastern margin of the SCS.

There exists another distinct NW- and WNW-trending fault set in this region. The majority of them cut through the early NE- and NNE-trending faults. Their formation was generally considered to be related to the later oblique collision between the Philippine Arc and the SCB, or the giant NW-trending strike-slip indentation and adjustment in the conjunction area of the PP and the EP. However, these NW-trending faults are easily misunderstood as the transform faults of the SCS.

Above all, the transform faults of the SCS are actually NNE-trending, as a portion of the NE- and NNE-trending strike-slip faults widely distributed in the continental shelf of the SCS (Ma *et al.*, 2014). In fact, they are also a natural extension of the NNE-trending right-lateral strike-slip faults in the SCB (Fig. 7). The pre-existing NE- and NNE-trending right-lateral strike-slip faults were reactivated by the collision between the Indian Plate and the EP in the Early Cenozoic, resulting in the opening of the SCS, and then the spreading process of the SCS, which was an oblique spreading, similar to the Red Sea. When the new oceanic crust emerged, the pre-existing faults evolved into the NNE-trending transform faults of the SCS. Moreover, Liu *et al.* (2016) identified a series of the dominant NE- and NNE-trending right-lateral strike-slip faults in seismic

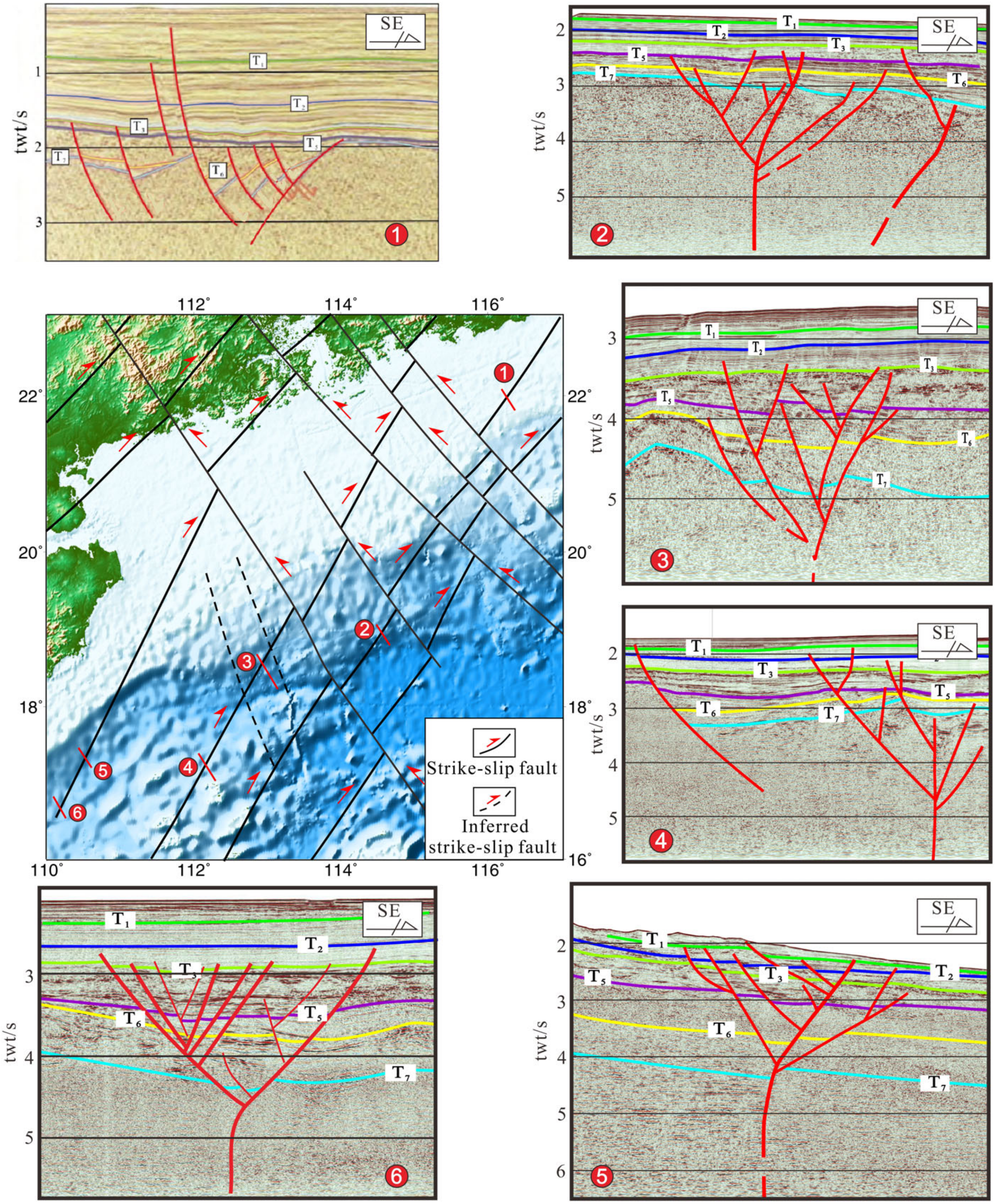

Figure 6. Basin-controlling strike-slip faults in the northern continental margin of the SCS and seismic profiles (modified from Wang *et al*., 2014). T7 interface represents the boundary between the pre-Mesozoic basement and the Cenozoic strata.

profiles of the OT, which controlled the stratigraphic succession and structural framework of the OT, inducing breakup of the volcanic island arcs and resulting in back-arc opening. Since the new oceanic crust emerged, the NE- and NNE-trending faults evolved into the transform faults of the OT. This directly indicates that the spreading of the OT and the opening of the SCS have the same geodynamic setting and a similar formation mechanism. They are all attributed to the right-lateral strike-slip process of the NE- and NNE-trending faults.

4.2. The SPVB: model of the IBM Trench NE- and NNE-trending retreat

A number of drilling cruises have been carried out since the start of the Ocean Drilling Program (ODP). The drilling results showed the KPR running through the middle of the PSP from north to south was the residual arc. Before about 30 Ma, the KPR and IBM island arcs were a unified island-arc system, without being separated. The DSDP 448 found that the volcanic activity of the KPR and adjacent area ceased in the period 32-31 Ma. The unified island-arc system began to break up at about this time (Jin, 1995).

Since the late Mesozoic, the main geodynamics of the PSP was driven by the motion of the PP (Li *et al*., 2013). Now the known oldest oceanic crust, about 150 Ma, in the Western Pacific was located to the east of the IBM Trench (Sdrolias *et al*., 2004). Corresponding to the palaeo-IBM Trench, the SPVB was a back-arc basin spreading during 30-17 Ma. The east of palaeo-IBM Trench has the older, colder, denser oceanic crust at that time than at present. So the subduction at the ancient trench can be compared with the present-day subduction. Shi and Wang (1993) argued, due to the older, colder and denser Western Pacific oceanic crust, the PP was easier to sink, resulting in high-angle subduction. The subducting plate further drives the trench to retreat, inducing the upwelling mantle flow and back-arc spreading. Their calculation results showed the trench retreating, and high-angle subduction contributed to induce the upwelling mantle flow and back-arc spreading. Meanwhile, they predicted by calculation that there should be the obvious upwelling mantle flow and back-arc spreading behind the IBM Trench, which was consistent with the current observations. Molnar and Atwater (1978) also made the point that the old oceanic crust was easier to sink with negative buoyancy, causing the trench to move seaward and leading to back-arc spreading. Zhong and Gurnis (1997) did a non-Newtonian fluid convection model with numerical simulation under the cylindrical coordinate, showing that it is possible to appear subduction rollback, and also described in detail the possible process of the subduction rollback.

Many plate reconstructions of the Western Pacific tectonics clearly demonstrate a large-scale NE- and NNE-trending slab rollback along the IBM Trench (Seno and Maruyama, 1984; Jolivet *et al*., 1989; Hall, 1997; Nichols and Hall, 1999; Honza and Fujioka, 2004; Sdrolias *et al*., 2004; Maruyama *et al*., 2009; Niu *et al*., 2015; Suo *et al*., 2015). Moreover, the IODP results also favour the triple junction of the Japan Trench, the Ryukyu Trench and the IBM Trench migrated from SW to NE-ENE (Haston and Fuller, 1991), which also confirmed that the IBM Trench did indeed move seaward to the PP (Zang and Ning, 2002).

Since the northern and western margins of the PSP separated from the EP with a subduction zone, the remote effect of the collision between the Indian Plate and the EP could not affect the PSP apparently. The SPVB developed parallel to the subduction zone, of which the magnetic lineations are substantially parallel to the residual arc of the KPR, indicating that the cause of the SPVB was back-arc rifting related to the PP subduction (Ren and Li, 2000; Honza and Fujioka, 2004). The most remarkable feature of the PP subduction was trench retreating in the Cenozoic (Zhang *et al*., 2016). Zhang and Shi (2003) pointed out that in the subduction rollback process, the underlying plate moved backward with the trench retreating, the stress state of the overlying plate shifted from compression to tension. The shifted stress state might lead to back-arc rifting. Based on the changed positions of the trench in the plate reconstruction of the marginal seas of the Western Pacific and nearby plates at four critical periods (45 Ma, 25 Ma, 15 Ma, present) (Jolivet *et al*., 1994), Ren and Li (2000) found that the extensional component of the deformation increased towards the back-arc zone, thus believing that the subduction rollback is one of the main formation mechanisms of back-arc spreading.

The transform fault is actually the movement track of the lithosphere on the surface of the Earth. According to the plate tectonics theory, the direction of transform faults of the back-arc basin resulting from subduction should be consistent with the direction of relative motion of the subducting plate. The back-arc spreading direction was approximately parallel to the direction of relative movement of oceanic plates (Honza and Fujioka, 2004). The NE- and ENE-directed retreat of the IBM Trench indicated the PP relative to the PSP moving northeastward and ENE-ward. According to the free space gravity anomalies and previous studies, the strikes of transform faults during the late spreading of the SPVB were NE- and ENE-trending, parallel to the relative motion sense of the PP to the PSP. This was in accordance with the plate tectonics theory.

The origin of the NE- and NNE-trending transform faults in the SPVB was the possible model of NE- and NNE-directed retreat of the IBM Trench. Because the older, colder, heavier Western Pacific oceanic crust was located to the east of the IBM Trench, there existed a high-angle subduction zone at the IBM Trench, driving the NE- and NNE-directed trench retreat due to wedge suction, inducing

DOI: 10.1002/gj

the upwelling mantle flow and resulting in the tensile stress on the surface of the overlying plate, named the PSP, further controlling the manner of the back-arc spreading. With the action of tensile stress, the palaeo-IBM Island Arc split, the back-arc basin began to spread and develop the NE- and NNE-trending transform faults. The transform faults were not perpendicular to the spreading ridge in the SPVB, on average about 26° to normal of the ridge (Table 1). It was another oblique spreading, not like the orthogonal spreading in a normal mid-oceanic ridge. This is a non-uniform spreading manner, with the emergence of complex magnetic lineation, nor progressive spreading.

In order to display the differences of the spreading in different segments of the back-arc basin, we have undertaken further work, separately measuring the angles between the transform faults and the normal of the ridges in the SB and the PVB (Table 1), and then calculated the mean value. Our results show that the measured average value (21.71°) in the SB was less than that (30.25°) in the PVB. This may be explained by the following two reasons: 1. The IBM Trench NE- and NNE-trending retreat may have had a different impact on the two basins. 2. The influence of the second (25 Ma-present) overall rotation of the PSP. It also highlights the complexity and the non-uniformity of the back-arc spreading.

4.3. The WPB (42-33 Ma): late-stage overall rotation model of the PSP

Due to the tectonic complexity of the PSP, the spreading process of the WPB was still not clear (Seno and Maruyama, 1984; Sasaki *et al*., 2014). Since the palaeo-IBM Trench subducted at about 54 Ma, the WPB developed on the southern side of the KPR.

According to whether there was an overlapping spreading centre in the projection of two contiguous rift valleys, Honza (1995) proposed three possible ideal modes for the marginal sea spreading. The first type has no overlapping spreading centre between two contiguous rift valleys. In contrast to the first type, the second has one overlapping spreading centre. The third was that the transform faults were perpendicular to the spreading axes of mid-oceanic ridges. Based on the angle between the transform faults and the normal line of the ridges, we tried to explore the spreading manner of the WPB and the formation mechanism of the current N–S-trending transform faults.

Table 1. The angles between the transform fault strikes and the normal of the ridge in the back-arc basins

Location		The angle between the transform faults and the normal of the ridge (°)			
		Measured value		Average value	
SPVB	SB	17.63	26.70	21.71	25.98
		24.09	18.40		
	PVB	27.56	33.34	30.25	
		28.50	31.59		
WPB		9.75	6.83	7.35	
		7.09	5.72		

By measuring and calculation, the angles between the nearly N–S-trending transform faults and the normal lines of the ridge at the early spreading stage (42-33 Ma) in the WPB were 7.35° on average (Table 1). The four measured values are close to each other, without much difference between them. The angle is very small. The near-N–S-trending transform faults were perpendicular to the E–W-trending spreading centre, similar to the normal mid-oceanic ridge. Concerning the probable impact of the second rotation stage since 25 Ma of the PSP, and the measurement method on the angle, this paper proposes that the spreading pattern at the late spreading stage of the WPB was similar to the normal mid-oceanic ridge, which was orthogonal spreading. It also coincides with the third type proposed by Honza (1995) (described above). Even the seafloor spreading occurred at normal mid-oceanic ridges, nor is it entirely orthogonal spreading. Nevertheless, some oblique spreading is suggested in most mid-oceanic ridges (Honza, 1995).

By comparing the different behaviours of the palaeo-IBM Trench retreat in the late spreading of the WPB and the SPVB, the oceanic crustal age differences of the subducting PP, whether the palaeo-KPR was parallel to the retreating trench, it indicated that the late spreading of the WPB also resulted from the palaeo-IBM Trench retreating. Seno and Maruyama (1984) also considered that the palaeo-IBM Trench retreating seaward led to the formation of the WPB and the SPVB. The formation and evolution of marginal seas in the Western Pacific show that the back-arc spreading was closely related to the motion of the surrounding plates (Honza, 1995). At about 42 Ma, the motion sense of the PP changed from NNW to WNW. To adjust to this change, the tectonic migration of the spreading centre of the WPB took place, and the spreading direction adjusted from N–S to NW–SE or NNW–SSE. All the above-mentioned evidence implies that WPB spreading was closely associated with the PP subduction and the retreat of the palaeo-IBM Trench. On the basis of the palaeomagnetic data, Hall (1996, 2002) carried out a plate reconstruction of the continental margin of Southeast Asia and the Western Pacific marginal seas, showing that the PSP did not rotate in the period 40-25 Ma while it proceeded about 40° clockwise rotation after 25 Ma. The WPB rotated together with the PSP. The near-N–S-trending transform faults that occurred at the early spreading stage of the WPB were rotated to become the current NE-trending, and the later NW- and NNW-trending transform faults were rotated to the present-day near-N–S or NNE trend.

The angles between the transform faults and the normal lines of the ridges can somehow reflect the marginal sea spreading manner. Therefore, by comparing these angles in different back-arc basins, we can explore the similarity and difference of the formation mechanism in different back-arc basins under a unified geodynamic setting. The back-arc spreading of the WPB and the SPVB was both related to the palaeo-IBM Trench retreat, which indicated the similarity of their formation mechanism. The angle (7.35°) between the near-N–S-trending transform faults and the normal lines of near-E–W-trending spreading axis was far less than that (25.98°) (Table 1) in the SPVB, reflecting the differences between their genetic mechanism. The small angle (7.35°) indicates that the late spreading stage (42-33 Ma) of the WPB was similar to that of the normal mid-oceanic ridge. It might be the case that the palaeo-IBM Trench retreated at the same rate relative to the palaeo-KPR. Moreover, it might reflect that the geodynamic setting of the whole PSP was relatively simple, without the obvious influence of the surrounding plates during the time after the spreading reorientation and before the spreading ceasing. This differed from the SPVB. The IBM Trench was not parallel to the KPR rifting in 30 Ma. The breakup of the KPR was non-uniform when the trench retreated.

4.4. Plate reconstruction: tectonic setting on the origin of transform faults in marginal seas of the Western Pacific

Some of most active marine research projects in the world at present are as follows: the International Ocean Discovery Program (IODP), International mid-oceanic ridge Project (InterRidge), International Continental Margin Program (InterMargins) and the Geodynamic Processes of Rifting and Subducting MarginS (GeoPRISMS), each of which focuses on the formation and evolution mechanism of marginal seas (Cawood, 2005; Li, 2008; Li *et al*., 2009a, b). These programmes are devoted to undertaking research on the time of opening, the closure time and the evolutionary processes of marginal seas, but seldom are they concerned with the genesis of transform faults. It is because of the unclear origin of transform faults that leads to the chaotic evolutionary history of marginal seas. So far, there have been plenty of plate reconstruction models about the formation and evolution of the Cenozoic marginal seas in the Western Pacific and the East Asian Continental Margin (Uyeda and Miyashiro, 1974; Hilde *et al*., 1977; Lee and Lawver, 1995; Sengor and Natalin, 1996; Yin and Nie, 1996; Maruyama *et al.,* 1997; Hall, 2002, 2012; Honza and Fujioka, 2004; Sdrolias *et al*., 2004; Whittaker *et al.,* 2007; Yin, 2010; Seton *et al.,* 2012). Substantial foundation work has been done already, and relatively reasonable plate reconstruction models have been put forward from the insights gained from studies of palaeomagnetism, magnetic lineation, geochemistry, sedimentary formation, structural connections, etc. However, each plate reconstruction had its own limitations. These reconstructions relied mostly on a single geophysical method; the geological evidence was insufficient, and thus different conclusions might be reached from different perspectives because of the multiplicity of geophysical inversion. In addition, the geomagnetic anomaly in the back-arc basin was especially weak and rather disorganized for the reasons of asymmetric spreading, mid-oceanic ridge transition and the intraplate volcanism after the spreading, which created a major challenge for the most precise redefinition of the magnetic lineation, reducing the accuracy of the marginal sea spreading process judged by magnetic lineation. Differences in these plate reconstructions showed not only the complexity of the formation and evolution of marginal seas in the Western Pacific but also the great controversies and contradictions.

Based on the preliminary results and understandings mentioned above, and the many previous studies on the Western Pacific marginal seas (Hall *et al*., 1995a, b, c; Hall, 1996, 1997, 2002; Honza and Fujioka, 2004; Sdrolias *et al*., 2004), this paper modified their previous plate reconstructions from the point of transform faults to make them more reasonable.

4.4.1. Early Eocene (51 Ma) (Fig. 7A)

In the Early Eocene, the Oki-Daito Ridge and the Amami Plateau in the northern PSP and the Halmahera Island in the southern PSP in their present-day positions were the old residual oceanic crust in the Western Pacific region (Hall, 1996, 2002). Based on palaeomagnetism and palaeolatitude data, the PSP was in a sub-equatorial position (Louden, 1977; Kinoshita, 1980; Hall *et al*., 1995a, b, c), showing the subsequent rotation process and the change of palaeolatitude (Hall, 2002). At this time, there was a spreading centre between the Indian Plate and the Australian Plate, which showed the relative independence of each other. At the same time, the Indian Plate began to collide with the southern margin of the EP. Also, there was a west-dipping subduction zone along the East Asian Continental Margin, extending southward to the Luzon Arc, and the northern and western Sulawesi Arc (Hall, 2002). At about 54 Ma, the massive boninitic volcanic rocks intruded into the present-day eastern margin of the PSP, initiating the IBM Arc (Hall, 2002). The WPB began to spread behind the arc and rotated clockwise, producing the rudiment of the PSP. The island of Borneo might have formed in the Late Cretaceous, and it was in its present-day geographic location from the Early Eocene following a clockwise rotation of 40° (Fuller *et al*., 1999; Zheng *et al*., 2016).

4.4.2. Middle Eocene (42 Ma) (Fig. 7B)

In the Middle Eocene, the Wathon mid-oceanic ridge spreading ceased, and the Indian Plate and the Australian Plate became one single plate, named the India-Australia Plate, moving northward rapidly (Hall, 2002). The WPB became wider, and its spreading system propagated through the Celebes Sea into the Makassar Strait (Hall, 1996). Because the WPB was surmised to have had an approximately 50° clockwise rotation in the 50-40 Ma interval, there might be enormous strike-slip faults between the PP and the Australian Plate, and the western margin of the PSP. At the eastern margin of the PSP, extensive island arcs were exposed, and the southern part of KPR continued to develop southward due to the subduction of the PP (Honza and Fujioka, 2004). At *ca.* 45 Ma, the proto-SCS started to subduct southward, producing a new and important accretion-type active continental margin extending from Sabah (Borneo) via the Sulu Arc into the Luzon Arc (Hall, 2002). The latter author considered that the slab-pull forces from the proto-SCS resulted in the spreading of the SCS. This conflicts with the observed geological facts in the East Asian Continental Margin. In contrast, we consider the spreading of the SCS was mainly due to the pull-apart effects controlled by the NNE-trending dextral strike-slip faults. At *ca.* 42 Ma, the strike of the Hawaii-Emperor Ridge changed, indicating a change of motion sense of the PP from NNW to WNW (Suo *et al.*, 2012; Li *et al.*, 2013). As a result, approximately 42 Myr ago, there was a major period of plate reorganization in this area. The subsequent ridge jump in the WPB might also be associated with this change. In the Late Eocene, the subduction of the PP was supposed to have resulted in the breakup of the eastern IBM Arc to generate the Caroline Sea at the eastern margin of the PSP (Hall, 2002), as proposed in Karig's model (Karig, 1974) for arc evolution. Because of the little knowledge concerning the Caroline Plate, the spreading direction of the Caroline Sea is very controversial.

4.4.3. Early Oligocene (34 Ma) (Fig. 7C)

The plate tectonic framework in the Early Oligocene was similar to that in the late Middle Eocene (40 Ma). At about 35 Ma, the spreading of the WPB ceased (Hilde and Lee, 1984; Honza and Fujioka, 2004; Li *et al.*, 2013). The subduction at the northern margin of the Borneo-Luzon Arc continued to consume the oceanic crust of the proto-SCS and formed the massive accretionary complex in northern Borneo (Hall, 1996, 2002). Honza and Fujioka (2004) suggested that the opening of the SCS was possibly activated by the approach of the spreading axis of the WPB, which was also different from our model. The SCS began to spread at about 34 Ma. On account of the subduction rollback, the palaeo-IBM Arc began to split and form the SPVB at approximately 30 Ma. Moreover, there was a north-dipping subduction zone all along the SE Asian margin in the earliest Oligocene or the latest Eocene.

4.4.4. Early Miocene (23 Ma) (Fig. 7D)

It was in the Late Oligocene or Early Miocene, at *ca.* 25 Ma, that the plate boundaries had the most significant changes (Hall *et al.*, 1995b, c; Sdrolias *et al.*, 2004). The PSP started its second clockwise rotation at this time (Hall, 2002). Many island arcs became effectively coupled to the PP. It started to become an intra-oceanic subduction zone at the eastern margin of the PSP, at which the PP subducted rapidly, and the rapid rollback of the trench hinge from this time (Hall, 2002). Hall also argued that the SPVB opened in a similar way with the Caroline Sea, which was a progressive spreading, and the SPVB was parallel to the subduction zone. However, according to the previous analysis, we believe that the NE- or NNE-directed subduction rollback at the IBM Trench led to the opening of the SPVB. The spreading stage of the Japan Sea was confirmed during the period 24-17 Ma, based on the ages of the seafloor rock (Tamaki *et al.*, 1992). We adopted the opinion of Jolivet *et al.* (1994) and Yin (2010) that the opening of the Japan Sea was controlled by the dextral strike-slip motion and further believe that the spreading of the SCS was also related to the giant dextral strike-slip faults (Xu *et al.*, 2014). The two marginal seas were similar in their formation.

4.4.5. Middle Miocene (16 Ma) (Fig. 7E)

In the Middle Miocene because of the rotation of the PSP and the probable strike-slip motion, its western boundary was fairly complex. There was a minor subduction zone within the Philippines on the basis of the distribution of isotopic ages and volcanic activity (Hall, 2002). The Caroline Plate rotated clockwise continuously as did the PSP. With the ongoing subduction, the oceanic crust of the proto-SCS north of Borneo was almost consumed completely (Luan and Zhang, 2009). The spreading of the SPVB east of the PSP ceased in the earliest Middle Miocene, about 17-15 Ma (Briais *et al.*, 1993; Okino *et al.*, 1998, 1999; Sdrolias *et al.*, 2004; Yin, 2010). The Ayu Trough at the southern edge of the PSP was initiated to spread slowly (Hall, 2002). At about 16 Ma, owing to the joint effect of the Australian Plate moving northward to collide with the southeastern Asian Continental Margin (Li *et al.*, 2012) and the blocking of the Dangerous Block subducting beneath Borneo (Luan and Zhang, 2009; Hui *et al.*, 2016a), the spreading of the SCS ceased and began to be subducted into the Philippines. Then the MT appeared (Li *et al.*, 2013). At the same time, the Nankai Trough, the Ryukyu Trench and the Luzon Trench developed, but their subduction rates might have been very slow, as deduced from the

DOI: 10.1002/gj

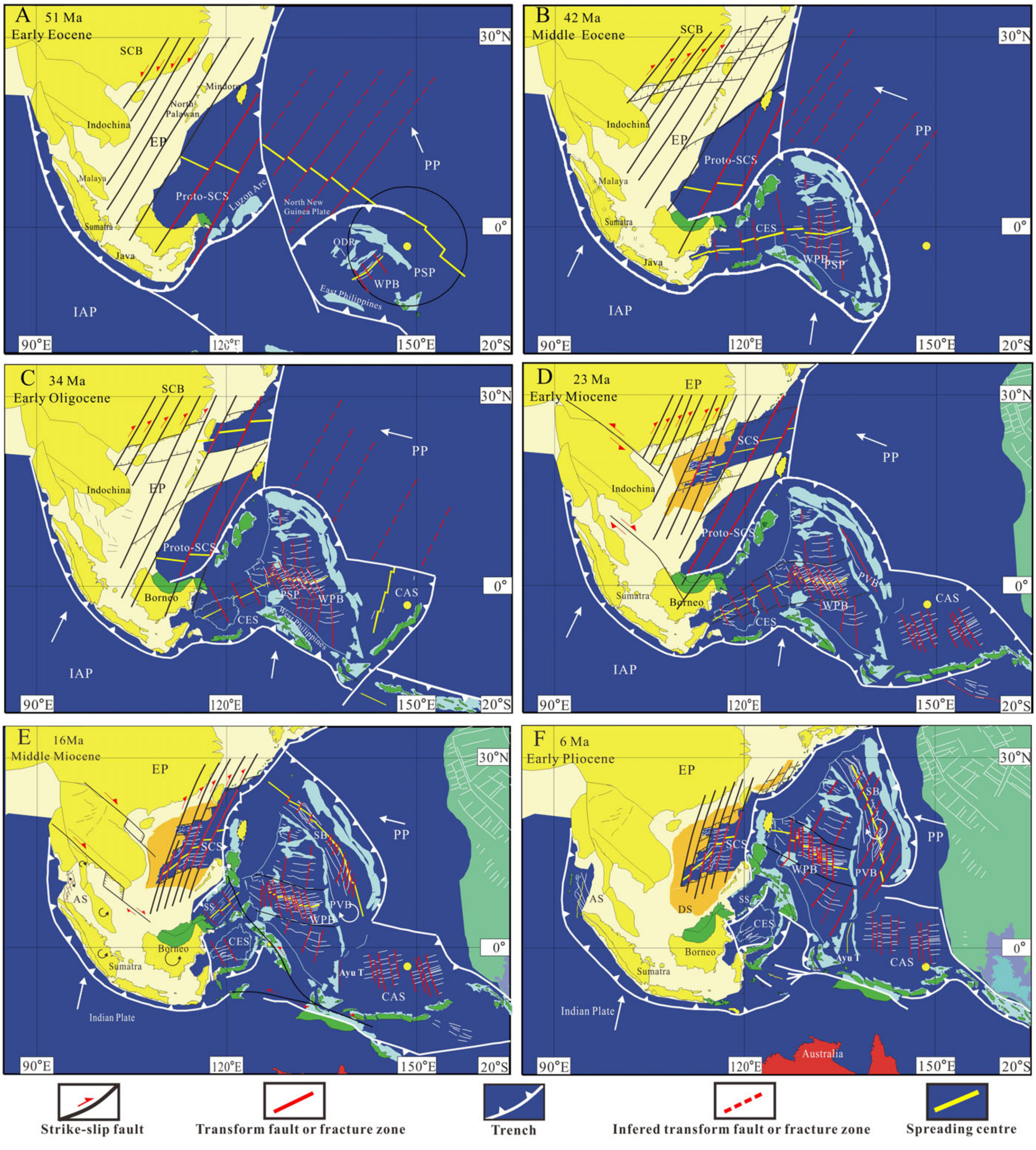

Figure 7. Revised plate reconstructions of Southeast Asia and the Pacific Plate in the Cenozoic (revised from Hall, 1996, 1997, 2002). IAP = India-Australia Plate; AS = Andaman Sea; Ayu T = Ayu Trough; DS = Dangerous Block; see Figure 1 for other abbreviations. Pacific Plate is shown in turquoise. Areas filled with green are mainly arc, ophiolitic and accreted material formed at plate margins. Areas filled in cyan and pale mauve are submarine arcs, and oceanic plateau. Pale yellow represents submarine parts of the Eurasian continental margins. Dark yellow represents deeper areas of the South China Sea. The red region represents Australia.

rotation rates of the Philippines at this stage (Honza and Fujioka, 2004).

4.4.6. Early Pliocene (6 Ma) (Fig. 7F)

The PSP moved towards the East Asian Continental Margin in a WNW direction, the PSP subducted westward into the Philippines, finally producing the Philippine Trench in the latest Miocene or the earliest Pliocene, at 6 or 4 Ma (Seno *et al*., 1993; Hall *et al*., 1995b; Honza and Fujioka, 2004). The Mariana Arc began to split in the Early Pliocene, forming the west and east Mariana Arc and the Mariana Trough in the later phase of this stage (Honza and Tamaki, 1985; Taylor, 1992), at approximately 3.5 Ma (Yamazaki *et al*., 1993). The oceanic crust developed in the southern OT at 2 Ma (Liu *et al*., 2016). The current plate tectonic configuration is then basically formed.

5. CONCLUSIONS

Based on the high-resolution tectonomorphology, gravity and magnetic anomalies, patterns of magnetic lineation, combined with regional geological setting, and the inheritance of tectonic activity, this paper selects the SCS, OT, WPB and SPVB as key basins to re-examine the distribution of transform faults. Furthermore, from the insight provided by the study of the strikes of transform faults, this paper reanalyzes the spreading manner of the marginal seas, improves the previous plate reconstruction model and proposes three models on the formation of the NNE-trending transform faults in back-arc basins.

(1) The model of inheriting the orientation of the strike-slip faults at the rifting continental margin from those in the adjacent region. The real strikes of transform faults should be NNE-trending rather than the traditionally-known NW-trending. The NNE-trending transform faults were actually the NNE-trending right-lateral strike-slip faults widely distributed in the continental shelf of the SCS, also being a natural extension of the NNE-trending right-lateral strike-slip faults in the SCB. The geodynamics of the OT spreading resembled that in the SCS. Therefore, the transform faults of the OT should also be NNE-trending. The transform faults are not perpendicular to the spreading axis, which display an oblique spreading.

(2) The model of the IBM Trench retreat to the NE and NNE. The NE- and NNE-trending retreat of the IBM Trench produced the NE- and NNE-directed horizontal tensile stress, which resulted in the KPR splitting, rifting, and then controlling the spreading process of the SPVB and the NE- and NNE-trending transform faults. The transform faults were not perpendicular to the spreading axis, also presenting an oblique spreading.

(3) The model of the later overall rotation of the PSP. The later spreading of the WPB formed the NW- and NNW-trending transform faults and an orthogonal spreading axis. Since 25 Ma, the WPB has been clockwise rotated by about 40° along with the overall rotation of the PSP. The near-N–S-trending transform faults during the early spreading of the WPB were rotated to become the present-day NE-trending ones, and the NW- and NNW-trending transform faults during the late spreading of the WPB were rotated to become the present-day near-N–S- or NNE-trending ones. Transform faults in the WPB were almost perpendicular to the spreading axis, similar to the normal ocean ridge spreading behaviour.

(4) Cenozoic transform fault in marginal seas is related to the subduction geodynamics of the Pacific Plate rather.

ACKNOWLEDGEMENTS

Research funding was provided by the NSFC project (grants 41325009, 41190072, 41502321, 41402172 and 41502185). This work was also financially supported by the National Programme on Global Change and Air-Sea Interaction, SOA (no. GASI-GEOGE-01) and Taishan Scholars Program and Aoshan Elite Scientist Plan to Prof. Sanzhong Li. We thank International Gravimetic Bureau (BGI) for providing free-air gravity data for the Philippine Sea Plate. And we are also grateful to two anonymous reviewers for their critical and constructive comments.

REFERENCES

Andrews, J.E. 1976. *Aspects of the geologic setting of manganese nodule deposits*. In: Glasby, G. P., Katz, H. R. (eds), Proceedings, Technical Bulletin No. 2, CCOP/SOPAC-IDOE Workshop, Suva, Fiji, **197**, 1–13.

Andrews, J.E. 1980. Morphologic evidence for reorientation of sea-floor spreading in the WPB. *Geology* **8**, 140–143.

ArRajehi, A., **McClusky, S.**, **Reilinger, R.**, **Semih, E.**, **Francisco, G.**, **Jamal, S.**, **Firyal, B.**, **Ghebrebrhan, O.**, **Biniam, H.**, **Shimelles, F.**, **Laike, A.**, **Salah, M.**, **Ali, R.**, **Rebecca, B.**, **Lewis, K. 2010**. Geodetic constraints on present-day motion of the Arabian Plate: implications for Red Sea and Gulf of Aden rifting. *Tectonics* **29**, 449–463.

Bellahsen, N., **Faccenna, C.**, **Funiciello, F.**, **Daniel, J.M.**, **Jolivet, L. 2003**. Why did Arabia separate from Africa? Insights from 3-D laboratory experiments. *Earth and Planetary Science Letters* **216**, 365–381.

Briais, A., **Patriat, P.**, **Tapponnier, P. 1993**. Updated interpretation of magnetic anomalies and sea floor spreading stages in the South China Sea: implications for the tertiary tectonics of Southeast Asia. *Journal Geophysical Research* **98**, 6299–6328.

Cawood, P.A. 2005. Terra Australis Orogen: Rodinia breakup and development of the Pacific and lapetus margins of Gondwana during the Neoproterozoic and Paleozoic. *Earth-Science Reviews* **69**, 249–279.

Chen, J., Wen, N. 2010. Landform and physiognomy. In: *The South China Sea Geophysical Atlas*, Chen, J., Wen, N. (eds). Science Press: Peking; 1–8 (in Chinese).

Cheng, S.X., **Li, S.Z.**, **Suo, Y.H.**, **Liu, X.**, **Yu, S.**, **Dai, L.M.**, **Ma, Y.**, **Zhao, S.J.**, **Wang, X.F.**, **An, H.T.**, **Xiong, L.J.**, **Xue, Y.C. 2012**.

Cenozoic tectonics and dynamics of basin of the Northern South China Sea. *Marine Geology and Quaternary Geology* **32**, 79–93 (in Chinese with English abstract).

Dai, L.M., Li, S.Z., Lou, D., Lin, X., Suo, Y.H., Yu, S. 2014. Numerical modeling of Late Miocene tectonic inversion in the Xihu Sag, East China Sea Shelf Basin, China. *Journal of Asian Earth Sciences* **86**, 25–37.

Deschamps, A., Lallemand, S. 2002. The WPB: an Eocene to early Oligocene back arc basin opened between two opposed subduction zones. *Journal of Geophysical Research, [Atmospheres]* **107**, 2322–2346.

Deschamps, A., Lallemand, S.E., Domingez, S. 1999. The last spreading episode of the WPB revisited. *Geophysical Research Letters* **26**, 2073–2076.

Deschamps, A., Okino, K., Fujioka, K. 2002. Late amagmatic extension along the central and eastern segments of the WPB fossil spreading axis. *Earth and Planetary Science Letters* **203**, 277–293.

Dewey, J., Cande, S., Pitman, W.C. 1989. Tectonic evolution of the Indian/Eurasia Collision Zone. *Eclogae Geologicae Helvetiae* **82**, 717–734.

Fu, Q.J., Cai, Z.R., Ma, C. 2007. Some comments on the formation and evolution of the South China Sea. *Marine Geology Letters* **9,** 1–7 (in Chinese with English abstract).

Fujioka, K., Kanamatsu, T., Ohara, Y., Fujimto, H., Okino, K., Tamura, C., Lallemand, S.E., Deschamps, B.A., Barretto, J.A., Togashi, N., Yamanobe, H., So, A. 2000. Parece Vela Rift and Central Basin Fault revisited—STEPS-IV (structure, tectonics and evolution of the Philippine Sea)—cruise summary report. *InterRidge News* **9**, 18–22.

Fujioka, K., Okino, K., Kanamatsu, T., Ohara, Y., Ishizuka, O., Haraguchi, S., Ishii, T. 1999. An enigmatic extinct spreading centre in the West Philippine backarc basin unveiled. *Geology* **27**, 1135–1138.

Fujiwara, T., Tamaki, K., Fujimoto, H., Ishii, T., Seama, N., Toh, H. 1995. Morphological studies of the Ayu trough, Philippine Sea-Caroline plate boundary. *Geophysical Research Letters* **22**, 109–112.

Fuller, M., Ali, J.R., Moss, S.J., Frost, G.M., Richter, B., Mahfi, A. 1999. Paleomagnetism of Borneo. *Journal of Asian Earth Sciences* **17**, 3–24.

Gerya, T. 2010. Dynamical instability produces transform faults at mid-ocean ridges. *Science* **329**, 1047–1050.

Gerya, T. 2012. Origin and models of oceanic transform faults. *Tectonophysics* **522**, 34–54.

Hall, R. 1996. Reconstructing Cenozoic SE Asia. *Geological Society of London Special Publications* **106**, 153–184.

Hall, R. 1997. Cenozoic plate tectonic reconstructions of SE Asia. *Geological Society London Special Publications* **126**, 11–23.

Hall, R. 2002. Cenozoic geological and plate tectonic evolution of SE Asia and the SW Pacific: computer-based reconstructions, model and animations. *Journal of Asian Earth Science* **20**, 353–431.

Hall, R. 2012. Late Jurassic-Cenozoic reconstruction of the Indonesian region and the Indian Ocean. *Tectonophysics* **570-571**, 1–41.

Hall, R., Ali, J.R., Anderson, C.D. 1995a. Cenozoic motion of the Philippine Sea Plate: paleomagnetic evidence from eastern Indonesia. *Tectonics* **14**, 1117–1132.

Hall, R., Ali, J.R., Anderson, C.D., Baker, S.J. 1995b. Origin and motion history of the Philippine Sea Plate. *Tectonophysics* **251**, 229–250.

Hall, R., Fuller, M., Ali, J.R., Anderson, C. 1995c. The Philippine Sea Plate: magnetism and reconstructions. In: *Active Margins and Marginal Basins of the Western Pacific*, Taylor, B., Natland, J. (eds). AGU: Washington, DC; 371–404.

Haston, R.B., Fuller, M. 1991. Paleomagnetic data from the Philippine Sea Plate and their tectonic significance. *Journal of Geophysical Researches* **4**, 6073–6098.

Hilde, T.W.C., Lee, C.S. 1984. Origin and evolution of the West Philippine Basin: a new interpretation. *Tectonophysics* **102**, 85–104.

Hilde, T.W.C., Uyeda, S., Kroenke, L. 1977. Evolution of the Western Pacific and its margin. *Tectonophysics* **38**, 145–165.

Holloway, N.H. 1982. North Palawan block, Philippines—its relation to Asian mainland and role in evolution of South China Sea. *Bulletin of American Association of Petroleum Geologists* **66**, 1355–1383.

Honza, E. 1995. Spreading mode of backarc basins in the Western Pacific. *Tectonophysics* **251**, 139–152.

Honza, E., Fujioka, K. 2004. Formation of arcs and back-arc basins inferred from the tectonic evolution of Southeast Asia since the Late Cretaceous. *Tectonophysics* **384**, 23–53.

Honza, E., Tamaki, K. 1985. The Bonin arc. In: *The Ocean Basins and Margins*, Nairn, A.E.M., Stehli, F.G., Uyeda, S. (eds), vol. **7A**. Plenum: New York; 459–502.

Huang, J., Zhao, D. 2009. Seismic imaging of the crust and upper mantle under Beijing and surrounding regions. *Physics of the Earth and Planetary Interiors* **173**, 330–348.

Hui, G.G., Li, S.Z., Guo, L.L., Zhang, G.X., Gong, Y.H., Somerville, I. D., Zhang, Y., Zheng, Q.L., Zang, Y.B. 2016a. Source and accumulation of gas hydrate in the northern margin of the South China Sea. *Marine and Petroleum Geology* **69**, 127–145.

Hui, G.G., Li, S.Z., Li, X.Y., Guo, L.L., Suo, Y.H., Somerville, I.D., Zhao, S.J., Hu, M.Y., Lan, H.Y., Zhang, J. 2016b. Temporal and spatial distribution of Cenozoic igneous rocks in the South China Sea and its adjacent regions: implications for tectono-magmatic evolution. *Geological Journal* **51(S1),** 429–447 DOI: 10.1002/gj2801.

Hutchison, C.S. 2010. Oroclines and palaeomagnetism in Borneo and South-East Asia. *Tectonophysics* **496**, 53–67.

Jin, X.C. 1995. Ocean drilling program and tectonics of the Western Pacific region. *Advances in Earth Science* **3**, 234–239 (in Chinese with English abstract).

Jolivet, L., Huchon, P., Rangin, C. 1989. Tectonic setting of Western Pacific marginal basins. *Tectonophysics* **160**, 23–47.

Jolivet, L., Tamaki, K. 1992. Neogene kinematics in the Japan Sea region and the volcanic activity of the northeast Japan arc. *Proceedings of the Ocean Drilling Program, Scientific Results* **127-128**, 1311–1331.

Jolivet, L., Tamaki, K., Fournier, M. 1994. Japan Sea, opening history and mechanism: a synthesis. *Journal of Geophysical Researches* **99**, 22237–22259.

Karig, D.E. 1971. Origin and development of marginal basins in the Western Pacific. *Journal of Geophysical Research* **76**, 2542–2561.

Karig, D.E. 1974. Evolution of arc systems in the Western Pacific. *Annual Review of Earth and Planetary Sciences* **2**, 51–75.

Karig, D.E. 1975. *Basin genesis in the Philippine Sea, Initial Reports of the Deep Sea Drilling Project 31*. U.S. Government Printing Office, Washington, D.C. 857–879.

Kinoshita, H., 1980. *Paleomagnetism of sediment cores from Deep Sea Drilling Project Leg 58, Philippine Sea*. *In*: Klein, G. dev., Kobayashi, K., Chamley, H., Curtis, D., Dick, H., Echols, D. J., Fountain, D. F., Kinoshita, H., Marsh, N. G., Mizuno, A., Nisterenko, G. V., Okada, H., Sloan, J. R., Waples, D., White, S. M. (Eds), Initial Reports of Deep Sea Drilling Project Leg 58. U.S. Government. Printing Office Washington, DC, 765–768.

Lallem, S.E., Liu, C. 1997. Swath bathymetry reveals active arc-continent collision near Taiwan. *Eos, Transactions American Geophysical Union* **78**, 173–175.

Lee, C.S., Shor, G.G., Bibee, L.D., Lu, R.S., Hilde, T.W. 1980. OT: origin of a back-arc basin. *Marine Geology* **35**, 219–241.

Lee, T.Y., Lawver, L.A. 1995. Cenozoic plate reconstruction of South-east Asia. *Tectonophysics* **251**, 85–138.

Li, J.B. 2008. Introduction. In: *Evolution of China's Marginal Seas and Its Effect of Natural Resources*, Li, J.B. (ed.). China Ocean Press: Peking; 1–2 (in Chinese).

Li, J.B. 2011. Dynamics of the continental margins of South China Sea: scientific experiments and research progresses. *Chinese Journal of Geophysics* **54**, 2993–3003 (in Chinese with English abstract).

Li, J.B., Jin, X.L., Gao, J.Y. 2002. Studies on tectonic geomorphology in the Central Basin of the South China Sea. *Science in China (Series D)* **32**, 239–248 (in Chinese).

Li, S.T., Lin, C.S., Zhang, Q.M. 1998. Dynamic process of the periodic rifting and tectonic events since 10 Ma in the marginal basins north of the South China Sea. *Chinese Science Bulletin* **43**, 797–810.

Li, S.Z., Jin, C., Dai, L.M., Zhang, G.W. 2009a. Marine geodynamics—advances and perspectives of international oceanfloor-related observatory network and exploration technique system. *Marine Geology and Quaternary Geology* **29**, 131–143 (in Chinese with English abstract).

Li, S.Z., Suo, Y.H., Liu, X., Dai, L.M., Yu, S., Zhao, S.J., Ma, Y., Wang, X.F., Cheng, S.X., An, H.T., Xue, Y.C., Xiong, L.J., Cao, X.Z., Xu, L. Q. 2012. Basin dynamics and basin groups of the South China Sea. *Marine Geology and Quaternary Geology* **32**, 55–78 (in Chinese with English abstract).

Li, S.Z., **Yu, S.**, **Zhao, S.J.**, **Liu, X.**, **Gong, S.Y.**, **Suo, Y.H.**, **Dai, L.M.**, **Ma, Y.**, **Xu, L.Q.**, **Cao, X.Z.**, **Wang, P.C.**, **Sun, W.J.**, **Yang, Z.**, **Zhu, J.J. 2013**. Tectonic transition and plate reconstructions of the East Asian continental margin. *Marine Geology and Quaternary Geology* **33**, 65–94 (in Chinese with English abstract).

Li, S.Z., Zhang, G.W., Liu, B.H. 2009b. Marine geodynamics from mid-oceanic ridge system to subduction factory. *Journal of Northwest University Science* **39,** 434–443 (in Chinese with English abstract)**.**

Liang, R.C., Wang, S.G., Wu, J.L. 2001. Preliminary study on geophysical field and the new crust in the middle of the OT. *Marine Geology and Quaternary Geology* **21**, 57–64 (in Chinese with English abstract).

Liao, J., **Gerya, T. 2014**. From continental rifting to seafloor spreading: insight from 3D thermo-mechanical modeling. *Gondwana Research* **29**, 1329–1343.

Lin, C.S., Ga, J.Y., Yu, X.J., Ye, F., Tan, Y.H. 2006. Characteristics of tectonic movement in the northern part of South China Sea during the Cenozoic. *Acta Oceanologica Sinica* **28**, 81–86 (in Chinese with English abstract).

Lin, J.H. 1999. The neotectonic deformation mechanism of Qilianshan Structure Belt. *China Journal of Seismology* **19**, 57–61 (in Chinese with English abstract).

Liu, B., **Li, S.Z.**, **Suo, Y.**, **Li, G.X.**, **Dai, L.M.**, **Somerville, I.D.**, **Guo, L. L.**, **Zhao, S.J.**, **Yu, S. 2016**. The geological nature and geodynamics of the Okinawa Trough, West Pacific. *Geological Journal* **51(S1),** 416–428 DOI: 10.1002/gj2774

Liu, M., **Cui, X.**, **Liu, F. 2004**. Cenozoic rifting and volcanism in eastern china: a mantle dynamic link to the Indo-Asian collision. *Tectonophysics* **393**, 29–42.

Liu, X., **Zhao, D.P.**, **Li, S.Z. 2013**. Seismic imaging of the Southwest Japan arc from the Nankai trough to the Japan Sea. *Physics of Earth and Planetary Interiors* **216**, 59–73.

Liu, X., **Zhao, D.P.**, **Li, S.Z. 2014**. Seismic attenuation tomography of the Northeast Japan arc: insight into the 2011 Tohoku earthquake (Mw 9.0) and subduction dynamics. *Journal of Geophysical Research-Solid Earth* **119**, 1094–1118.

Louden, K.E. 1977. Paleomagnetism of DSDP sediments, phase shifting of magnetic anomalies, and rotation of the West Philippine Basin. *Journal of Geophysical Research* **82**, 2989–3002.

Loureneo, N., **Miranda, J.M.**, **Luis, J.F.**, **Ribeiro, A.**, **Mendes, V.L.A.**, **Madeira, J.**, **Needham, H.D. 1998**. Morpho-tectonic analysis of the Azores Volcanic Plateau from a new bathymetric compilation of the area. *Marine Geophysical Researches* **20**, 141–156.

Luan, X.W., Zhang, L. 2009. Tectonic evolution modes of South China Sea: passive spreading under complex actions. *Marine Geology and Quaternary Geology* **29**, 59–74 (in Chinese with English abstract).

Luyendyk, B. 1969. *Geological and geophysical observations in an abyssal hill area using a deeply towed instrument package.* |Ph.D.dissert. |: San Diego, California, University of San Diego, 212p.

Ma, Y., **Li, S.Z.**, **Liu, X.**, **Zhao, S.J.**, **Yu, S.**, **Wang, X.F.**, **Zhang, B.K. 2014**. Formation mechanism of the Beibuwan Basin, South China Sea. *Journal of Jilin University (Earth Science Edition)* **44**, 1727–1736.

Maruyama, S., **Hasegawa, A.**, **Santosh, M.**, **Kogiso, T.**, **Omori, S.**, **Nakamura, H.**, **Kawai, K.**, **Zhao, D. 2009**. The dynamics of big mantle wedge, magma factory, and metamorphic-metasomatic factory in subduction zones. *Gondwana Research* **16**, 414–430.

Maruyama, S., **Isozaki, Y.**, **Kimura, G.**, **Terabayashi, M. 1997**. Paleogeographic maps of the Japanese Islands: plate tectonic synthesis from 750 Ma to the present. *The Island Arc* **6**, 121–142.

Molnar, P., **Atwater, T. 1978**. Interarc spreading and cordilleran tectonics as alternates related to the age of subducted oceanic lithosphere. *Earth and Planetary Science Letters* **441**, 330–340.

Mrozowski, D.L., **Hayes, D.E. 1982**. The evolution of the Parece Vela Basin, Eastern Philippine Sea. *Earth and Planetary Science Letters* **46**, 49–67.

Nichols, G., **Hall, R. 1999**. History of the Celebes Sea Basin based on its stratigraphic and sedimentological record. *Journal of Asian Earth Sciences* **17**, 47–59.

Niu, Y.L., **Liu, Y.**, **Xue, Q.Q.**, **Shao, F.L.**, **Chen, S.**, **Duan, M.**, **Guo, P. Y.**, **Gong, H.M.**, **Hu, Y.**, **Hu, Z.X.**, **Juanjuan Kong, J.J.**, **Li, J.Y.**, **Liu, J.J.**, **Sun, P.**, **Sun, W.L.**, **Ye, L.**, **Xiao, Y.Y.**, **Zhang, Y. 2015**. Exotic origin of the Chinese continental shelf: new insights into the tectonic evolution of the Western Pacific and eastern China since the Mesozoic. *Science Bulletin* **60**, 1598–1616.

Okino, K., **Fujioka, K. 2003**. The Central Basin spreading center in the Philippine Sea: structure of an extinct spreading center and implications for marginal basin formation. *Journal of Geophysical Research* **108**, 1–18.

Okino, K., **Kasuga, W.**, **Ohara, Y. 1998**. A new scenario of the Parece Vela Basin genesis. *Marine Geophysical Researches* **20**, 21–40.

Okino, K., **Ohara, Y.**, **Kasuga, S.**, **Kato, Y. 1999**. The Philippine Sea: new survey results reveal the structure and the history of the marginal basins. *Geophysical Research Letters* **26**, 2287–2290.

Oshima, S., **Takanashi, M.**, **Kato, S.**, **Uchida, M.**, **Okazaki, I.**, **Kasuga, S.**, **Kawashiri, C.**, **Kaneko, Y.**, **Ogawa, M.**, **Kawai, K.**, **Seta, H.**, **Kato, Y. 1988**. Geological and geophysical survey in the OT and the adjoining seas of Nansei Kyoto. *Report of Hydrographic Research Japan* **24**, 19–44.

Packham, G.H., **Falvey, D.A. 1971**. An hypothesis for the formation of marginal seas in the Western Pacific. *Tectonophysics* **11**, 79–109.

Püthe, C., **Gerya, T. 2014**. Dependence of mid-ocean ridge morphology on spreading rate in numerical 3-D models. *Gondwana Research* **25**, 270–283.

Qu, C., Zhou, H.L., Zhao, D.P. 2007. Deep structure beneath the west margin of Philippine Sea Plate and South China Sea from P and S wave travel time tomography. *Chinese Journal of Geophysics* **50**, 1757–1768 (in Chinese with English abstract).

Queano, K., **Ali, J.R.**, **Milsom, J.**, **Aitchison, J.**, **Pubellier, M. 2007**. North Luzon and the Philippine Sea Plate motion model: insights following palaeomagnetic, structural, and age-dating investigations. *Journal of Geophysical Research, B: Solid Earth* **112b**(B5), 2637–2655.

Ren, J.Y., Li, S.T. 2000. Spreading and dynamic setting of marginal basins of the Western Pacific. *Earth Science Frontiers (China University of Geosciences, Beijing)* **7**, 203–213 (in Chinese with English abstract).

Sasaki, T., **Yamazaki, T.**, **Ishizuka, O. 2014**. A revised spreading model of the WPB. *Earth, Planets and Space* **66**, 1–9.

Sdrolias, M., **Roest, W.R.**, **Müller, R.D. 2004**. An expression of Philippine Sea plate rotation: the Parece Vela and Shikoku basins. *Tectonophysics* **394**, 69–86.

Sengor, A.M.C., **Natalin, B.A. 1996**. Paleotectonics of Asia: fragments of a synthesis. In: *The Tectonic Evaluation of Asia*, Yin, A., Harrison, M. (eds). Cambridge University Press: Cambridge; 487–614.

Seno, T., **Maruyama, S. 1984**. Paleogeographic reconstruction and origin of the Philippine Sea. *Tectonophysics* **1**, 53–84.

Seno, T., **Stein, S.**, **Gripp, A.E. 1993**. A model for the motion of the Philippine Sea Plate consistent with NUVEL-1 and geologic data. *Journal Geophysical Research* **98**, 17941–17948.

Seton, M., **Muller, R.D.**, **Zahirovic, S.**, **Gaina, C.**, **Torsvik, T.**, **Shephard, G.**, **Talsma, A.**, **Gurnis, M.**, **Maus, S.**, **Chandler, M. 2012**. Global continental and ocean basin reconstruction since 200 Ma. *Earth-Science Reviews* **113**, 212–270.

Shi, X.F., Yan, Q.S. 2013. Magmatism of typical marginal basins (or back-arc basins) in the West Pacific. *Advances in Earth Science* **28,** 737–750 (in Chinese with English abstract).

Shinjo, R., **Kato, Y. 2000**. Geochemical constrains on the origin of bimodal magmatism at the Okinawa Trough, an incipient back-arc basin. *Lithos* **54**, 117–137.

Sleep, N.H., **Toksoz, M.N. 1971**. Evolution of marginal basins. *Nature* **33**, 548–550.

Suo, Y.H., **Li, S.Z.**, **Dai, L.M.**, **Liu, X.**, **Zhou, L.H. 2012**. Cenozoic tectonic migration and basin evolution in East Asia and its continental margins. *Acta Petrologica Sinica* **28**, 2602–2618 (in Chinese with English abstract).

Suo, Y.H., **Li, S.Z.**, **Zhao, S.J.**, **Somerville, I.D.**, **Yu, S.**, **Dai, L.M.**, **Xu, L.Q.**, **Cao, X.Z.**, **Wang, P.C. 2015**. Continental margin basins in East Asia: tectonic implications of the Meso-Cenozoic East China Sea pull-apart basins. *Geological Journal* **50**, 139–156.

Shi, Y.L., **Wang, Q.Y. 1993**. Roll-back subduction and back-arc opening.

Acta Geophysica Sinica **36**, 37–43 (in Chinese with English abstract).
Takahashi, N., **Kodaira, S.**, **Klemperer, S.L.**, **Tatsumi, Y.**, **Kaneda, Y.**, **Suyehiro, K. 2007**. Crustal structure and evolution of the Mariana intra-oceanic island arc. *Geology* **35**, 203–206.
Tamaki, K. 1995. Opening tectonics of the Japan Sea. In: *Backarc Basins: Tectonics and Magmatism*, Taylor, B. (ed). Plenum Press: New York; 407–419.
Tamaki, K., **Honza, E. 1991**. Global tectonics and formation of marginal basins: role of the Western Pacific. *Episodes* **14**, 224–230.
Tamaki, K., **Suyehiro, K.**, **Allan, J.**, **Ingle, J.C. Jr.**, **Pisciotto, K.A. 1992**. Tectonic synthesis and implication of Japan Sea ODP drilling. In: Tamaki, K., Suyehiro, K., Allan, J., McWilliams, M., *et al*., (eds). *Proceedings of the Ocean Drilling Program, Scientific Results* **127/128**, 1333–1348.
Taylor, B., **1992**. Rifting and volcanic-tectonic evolution of the Izu-Bonin-Mariana arc. *Proceedings of the Ocean Drilling Program, Scientific Results*, **126**, 627–651.
Taylor, B., Hayes, D.E. 1983. Origin and history of the South China Sea Basin. In: Hayes, D. E. (Ed.), *The Tectonic and Geologic Evolution of Southeast Asian Seas and Islands*. Geophysical Monograph, American Geophysical Union, 23–56.
Taylor, B., **Natland, J. 1995**. Active margin and marginal basin of the Western Pacific. *Geophysical Monograph, American Geophysical Union (Washington D.C.)* **88**, 56–88.
Tokuyama, H. 1995. Origin and development of the Philippine Sea. In: *Geology and Geophysics of the Philippine Sea*, Tokuyama, H., Sheheka, N., Isezaki, N. (eds). Terra Science Publisher: Tokyo; 155–163.
Uyeda, S., **McCabe, R. 1983**. A possible mechanism of episodic spreading of the Philippine Sea. In: *Accretion Tectonics in the Circum-Pacific Regions*, Hashimoto, M., Uyeda, S. (eds). Terra Science Publications: Tokyo; 291–306.
Uyeda, S., **Miyashiro, A. 1974**. Plate tectonic and Japanese islands: a synthesis. *Geological Society of American Bulletin* **85**, 1159–1170.
Wang, P.L., **Lo, C.H.**, **Chung, S.L.**, **Lee, T.Y.**, **Lan, C.Y.**, **Thang, T.V. 2000**. Onset timing of left-lateral movement along the Ailao Shan-Red River Shear Zone: $^{40}Ar/^{39}Ar$ dating constraint from the Nam Dinh Area, northeastern Vietnam. *Journal of Asian Earth Sciences* **18**, 281–292.
Wang, X.F., Yu, S., Gong, Y.H., Li, S.Z., Liu, X., Ma, Y., Zhao, S.J. 2014. Extension of NE-trending faults in South China to Northern South China Sea Continental Shelf. *Geotectonica et Metallogenia* **38**, 557–570 (in Chinese with English abstract).
Whittaker, J.M., **Müller, R.D.**, **Sdrolias, M.**, **Heine, C. 2007**. Sunda-Java trench kinematics, slab window formation and overriding plate deformation since the Cretaceous. *Earth and Planetary Science Letters* **255**, 445–457.
Wilson, J.T. 1965. A new class of faults and their bearing on continental drift. *Nature* **207**, 343–347.
Wu, S.G., Fan, J.K., Dong, D.D. 2013. Discussion on the tectonic division of the Philippine Sea Plate. *Geological Sciences* **48**, 677–692 (in Chinese with English abstract).
Xiong, L.J., **Li, S.Z.**, **Suo, Y.H.**, **Liu, X.**, **Yu, S.**, **Cheng, S.X.**, **Xue, Y.C.**, **An, H.T.**, **Dai, L.M.**, **Ma, Y.**, **Wang, X.F. 2012**. Cenozoic basin-controlling faults and their bearing on basin groups formation in the South China Sea. *Marine Geology and Quaternary Geology* **32**, 113–127 (in Chinese with English abstract).
Xu, J., **Avraham, B.Z.**, **Kelty, T.**, **Yu, H.S. 2014**. Origin of marginal basins of the NW Pacific and their plate tectonic reconstructions. *Earth Science Reviews* **130**, 154–196.
Xue, Y.C., **Li, S.Z.**, **Liu, X.**, **Suo, Y.H.**, **Dai, L.M.**, **Yu, S.**, **Zhao, S.J.**, **Wang, P.C.**, **Xiong, L.J.**, **An, H.T.**, **Cheng, S.X.**, **Wang, X.F.**, **Ma, Y. 2012**. Segmentation of subduction system in the Eastern South China Sea and dynamics of related basin groups. *Marine Geology and Quaternary Geology* **32**, 129–147 (in Chinese with English abstract).
Yamazaki, T., **Murakami, F.**, **Saito, E. 1993**. Mode of seafloor spreading in the northern Mariana Trough. *Tectonophysics* **221**, 207–222.
Yamazaki, T., **Takahashi, M.**, **Iryu, Y.**, **Sato, T.**, **Oda, M.**, **Takayanagi, H.**, **Chiyonobu, S.**, **Nishimura, A.**, **Nakazawa, T.**, **Ooda, T. 2010**. Philippine Sea Plate motion since the Eocene estimated from paleomagnetism of seafloor drill cores and gravity cores. *Earth, Planets and Space* **62**, 1–8.
Yan, Q.S., **Shi, X.F.**, **Wang, K.S.**, **Bu, W.R.**, **Xiao, L. 2008**. Major element, trace element, Sr-Nd-Pb isotopic studies of Cenozoic alkali basalts from the South China Sea. *Science in China (Series D)* **51**, 550–566.
Yeh, Y.C., **Sibuet, J.C.**, **Hsu, S.K.**, **Liu, C.S. 2010**. Tectonic evolution of the Northeastern South China Sea from seismic interpretation. *Journal of Geophysical Research* **115**, 258–273.
Yin, A. 2010. Cenozoic tectonic evolution of Asia: a preliminary synthesis. *Tectonophysics* **488**, 293–325.
Yin, A., **Nie, S.R. 1996**. A Phanerozoic palinspastic reconstruction of China and its neighbouring regions. In: *The Tectonic Evaluation of Asia*, Yin, A., Harrison, T.M. (eds). Cambridge University Press: Cambridge; 442–285.
Zang, S.X., Ning, J.Y. 2002. Interaction between Philippine Sea plate (PH) and Eurasia (EU) plate and its influence on the movement in Eastern Asia. *Chinese Journal of Geophysics* **45**, 188–197 (in Chinese with English abstract).
Zhang, B., Li, G.X., Li, S.Z., Dada, O.A. 2016. Docking and subduction of the West Pacific seamounts along the Mariana Trench and their effects. *Geological Journal* **51(S1),** 579–592 DOI: 10.1002/gj2760
Zhang, J., Shi, Y.L. 2003. Thermodynamics mechanism of the marginal extensional belt of East Asia. *Geotectonica et Metallogenia* **27**, 222–227 (in Chinese with English abstract).
Zhao, D.P., **Ohtani, E. 2009**. Deep slab subduction and dehydration and their geodynamic consequences: evidence from seismology and mineral physics. *Gondwana Research* **16**, 401–413.
Zheng, Q.L., **Li, S.Z.**, **Suo, Y.H.**, **Li, X.Y.**, **Guo, L.L.**, **Wang, P.C.**, **Zhang, Y.**, **Zang, Y.B.**, **Jiang, S.H.**, **Somerville, I.D. 2016**. Structures around the Tinjar-West Baram Line in northern Kalimantan and seafloor spreading in the Proto-South China Sea. *Geological Journal* **51(S1),** 513–523 DOI: 10.1002/gj2806.
Zhong, S., **Gurnis, M. 1997**. Dynamic interaction between tectonic plates, subducting slabs, and the mantle. *Earth Interactions* **3**, 1–18.
Zhou, D., Chen, H.Z., Wu, S.M., Yu, H.X. 2002. Opening of the South China Sea by dextral splitting of the East Asian Continental Margin. *Acta Geologica Sinica* **76**, 180–190 (in Chinese with English abstract).
Zhu, W.L., Mi, L.J. 2010. China Sea Area. In: *Atlas of Oil and Gas Basin, China Sea*. Petroleum Industry Press: Beijing; 3–20 (In Chinese).